# AN ASSESSMENT OF WINKLER MODEL FOR SIMULATION OF SHALLOW FOUNDATION UPLIFT

A THESIS SUBMITTED TO
THE GRADUATE SCHOOL OF NATURAL AND APPLIED SCIENCES
OF
MIDDLE EAST TECHNICAL UNIVERSITY

BY

REFİK BURAK TAYMUŞ

IN PARTIAL FULFILLMENT OF THE REQUIREMENTS
FOR
THE DEGREE OF MASTER OF SCIENCE
IN
ENGINEERING SCIENCES

JULY 2008

Approval of the thesis:

**AN ASSESSMENT OF WINKLER MODEL FOR SIMULATION OF SHALLOW FOUNDATION UPLIFT**

Submitted by **REFİK BURAK TAYMUŞ** in partial fulfillment of the requirements for the degree of **Master of Science in Engineering Sciences Department, Middle East Technical University** by,

Prof. Dr. Canan Özgen _____
Dean, Graduate School of **Natural and Applied Sciences**

Prof. Dr. Turgut Tokdemir _____
Head of Department, **Engineering Sciences**

Assist. Prof. Dr. Mustafa Tolga Yılmaz _____
Supervisor, **Engineering Sciences Dept., METU**

Assoc. Prof. Dr. Murat Dicleli _____
Co-Supervisor, **Engineering Sciences Dept., METU**

**Examining Committee Members:**

Prof. Dr. M. Ruşen Geçit _____
Engineering Sciences Dept., METU

Assist. Prof. Dr. M. Tolga Yılmaz _____
Engineering Sciences Dept., METU

Prof. Dr. Polat Saka _____
Engineering Sciences Dept., METU

Assoc. Prof. Dr. Murat Dicleli _____
Engineering Sciences Dept., METU

Assoc. Prof. Dr. Sadık Bakır _____
Civil Engineering Dept., METU

**Date:** July 28, 2008

**I hereby declare that all information in this document has been obtained and presented in accordance with academic rules and ethical conduct. I also declare that, as required by these rules and conduct, I have fully cited and referenced all material and results that are not original to this work.**

Name, Surname : Refik Burak Taymuş

Signature :

# ABSTRACT

AN ASSESSMENT OF WINKLER MODEL FOR SIMULATION OF FOUNDATION UPLIFT

Taymuş, Refik Burak

M.S., Department of Engineering Sciences

Supervisor: Assist. Prof. Dr. Mustafa Tolga Yılmaz

Co – Supervisor: Assoc. Prof. Dr. Murat Dicleli

July 2008, 53 pages

Foundation uplift is the partial separation of a shallow foundation from soil due to excessive load eccentricity. Foundation uplift can significantly change the seismic response of slender structures, and frames as well. In literature, different support models for foundations are employed in order to simulate foundation uplift in seismic analysis of structures. One of the most widely used models is the Winkler model which assumes distributed tensionless springs beneath a shallow foundation. In this study, two simple algorithms are developed in order to compute static and dynamic response of foundations on tensionless supports. Any formula given in literature for calculation of foundation impedance coefficients can be easily introduced in these algorithms. Hence, the use of Winkler model is critically evaluated through comparisons with the response of a foundation on elastic halfspace. For that purpose, available impedance formulas given for a shallow rectangular foundation on elastic halfspace are used. It is concluded that, the coupling between vertical displacement and rocking of foundation is very significant during uplift. Therefore, the accuracy of Winkler model in uplift

simulation is limited, since the model cannot simulate vertical and rocking response of a shallow foundation concurrently with a single spring coefficient.

**Keywords :** Foundation Uplift, Winkler Model, Tensionless Springs, Impedance, Elastic Half-space.

# ÖZ

TEMEL KALKMASI SİMÜLASYONU İÇİN WINKLER MODELİNİN BİR DEĞERLENDİRMESİ

Taymuş, Refik Burak
Yüksek Lisans , Mühendislik Bilimleri Bölümü
Tez Yöneticisi: Yrd. Doç. Dr. Mustafa Tolga Yılmaz
Ortak Tez Yöneticisi: Doç. Dr. Murat Dicleli

Temmuz 2008, 53 sayfa

Temel kalkması, aşırı yük eksantrikliği nedeniyle yüzeysel bir temelin zeminle temasının kısmen kaybolmasıdır. Temel kalkması narin yapıların ve çerçevelerin sismik davranışını belirgin şekilde değiştirebilir. Literatürde, deprem yüklerinin düşünüldüğü yapısal analizlerde temel kalkmasının benzetimini gerçekleştirebilmek için, çok sayıda temel desteği modeli verilmiştir. En yaygın olarak kullanılan modellerden biri, yüzeysel bir temel altında yayılı gerilimsiz yaylar olduğunu varsayan Winkler modelidir. Bu çalışmada, gerilimsiz destekler üzerindeki temellerin dinamik ve sismik tepkisini hesaplamak için iki basit algoritma geliştirilmiştir. Temel empedans katsayılarının hesabı için literatürde verilen herhangi bir formül bu algoritmalar içerisine kolaylıkla sokulabilir. Böylece, Winkler modelinin kullanımı, Winkler temelinin tepkisinin elastik yarı-uzay üzerindeki temelin tepkisiyle karşılaştırılması yoluyla eleştirilmiştir. Bu doğrultuda, elastik yarı-uzay üzerindeki sığ dikdörtgen temel için literatürde verilen empedans formülleri kullanılmıştır. Temelin dikey deplasmanı ve devrilme açısı arasındaki bağlantının kalkma esnasında çok önemli olduğu sonucuna varılmıştır. Bu yüzden, kalkma simülasyonundaki Winkler modelinin

doğruluğu çok sınırlıdır, çünkü model tek bir yay katsayısı ile sığ temelin düşey ve devrilme tepkisini aynı zamanda taklit edemez.

**Anahtar kelimeler :** Temel Kalkması, Winkler Modeli, Gerilimsiz Yaylar, Empedans, Elastik yarı-uzay.

# ACKNOWLEDGEMENTS

I offer my thanks to my supervisor Assist. Prof. Dr. Mustafa Tolga Yılmaz for the encouragement, help, support he gives to me and for his patience during this study.

I also thank to my friends who everytime support me throughout this study, especially Hakan Bayrak, Cengizhan Durucan, Serdar Çarbaş, Ferhat Erdal and Erkan Doğan.

I would like to offer to thank my parents Mesut Taymuş and Gülten Taymuş, my deary elder sister Elif Kırkkeseli and her husband Haluk Kırkkeseli. They have been my biggest supporter in my bad days. I know that also after this time they will continue to be so. I will try to deserve to them for my life.

# TABLE OF CONTENTS



## CHAPTERS

# LIST OF FIGURES

## FIGURES

# LIST OF TABLES

## TABLES

# CHAPTER 1

# INTRODUCTION

## 1.1 The significance of foundation uplift in engineering practice

Drained soils cannot resist tensile forces. Therefore, no suction (tensile stress) can occur beneath shallow foundations resting on drained soils. Severe seismic or wind loads, can induce large load eccentricity on shallow foundations, resulting in temporary separation of the foundation from soil. Hence, foundation uplift is the partial loss of contact between soil and foundation due to excessive vertical load eccentricity acting on foundation (Figure 1.1).

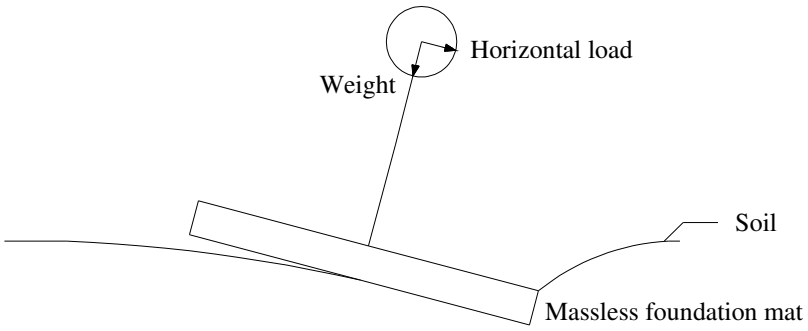


**Figure 1.1.** Uplift of a shallow foundation to bear excessive overturning moment exerted by an inversed pendulum structure.

Foundation uplift is particularly important for slender structures, such as towers,

chimneys and bridge piers, since the reduction in contact area between the soil and foundation can result in significant increase in support flexibility (Xu and Spyrakos, 1996; Mergos and Kavashima, 2005). The reduced stiffness of the soil-structure system may result in a significant increase in natural period of oscillations if foundation uplift is excessive. Depending on the frequency content of the ground motion, the shift in natural period during oscillations may induce significant deviations from the computed response for which no foundation uplift is presumed (Yim and Chopra, 1985; Roeder et al., 1996). Foundation uplift is particularly important for short-period structures, since the natural period of soil-structure system is more sensitive to foundation flexibility (Solomon et al., 1984; Celep and Güler, 1990; Psycharis, 1991). Furthermore, uplift can induce significant vertical displacements on structural response (Song and Lee, 1993).

Foundation uplift can also significantly modulate the distribution and level of damage on a frame (Huckelbridge and Clough, 1978; Roeder et al., 1996). Determination of load capacity and stiffness of a foundation is particularly important to find the structural elements that are most prone to damage, since uplifting of shallow foundations can provide additional nonlinearity into structural system. (Harden et al., 2006). Besides, seismic response of a shear wall within a frame depends on uplift response of its foundation (Anderson, 2002).

Therefore, realistic modeling of uplift is important for accurate calculation of structural response under seismic loading, when excessive load eccentricity is induced on shallow foundations. This study aims to develop algorithms for calculation of static and dynamic response of shallow foundations during uplift.

### 1.2. Literature Survey

Several simple models are employed in literature for practical modeling of foundation uplifts on soils which are presumed to behave linearly elastic. The simplest model is the one used by Yim and Chopra (1984) in order to investigate the effect of foundation uplift on structural response. In this model the shallow foundation is supported by a couple of spring and dashpot elements located on

each edge of rigid foundation (Figure 1.2.a). The second one is Winkler (foundation) model, in which distributed spring and dashpot elements bear loads acting on a rigid foundation (Figure 1.2.b). The Winkler model is used by several authors to simulate foundation uplift during seismic loading (e.g., Wolf and Skrikerud, 1978; Celep and Güler, 1990; Psycharis, 1991, 2007; Chen and Lai, 2002). Present a seismic design and analysis guidelines, such as ATC-40 and FEMA-356 (ATC, 1996; ASCE, 2000), recommend using Winkler model to calculate the stiffness of foundations during uplift (Harden et al., 2006). The third model is the S model (Figure 1.2.c), which is an improvement on the first model such that the response of Winkler model is simulated with best accuracy through adjusting the distance between the two spring elements (Song and Lee, 1993). However, the actual response of an elastic half-space can be significantly different from that of Winkler model. That is why foundation impedance factors presented by Gazetas (1991) is employed in seismic design practice, instead of employing Winkler model, when foundation uplift is none of engineering concern.

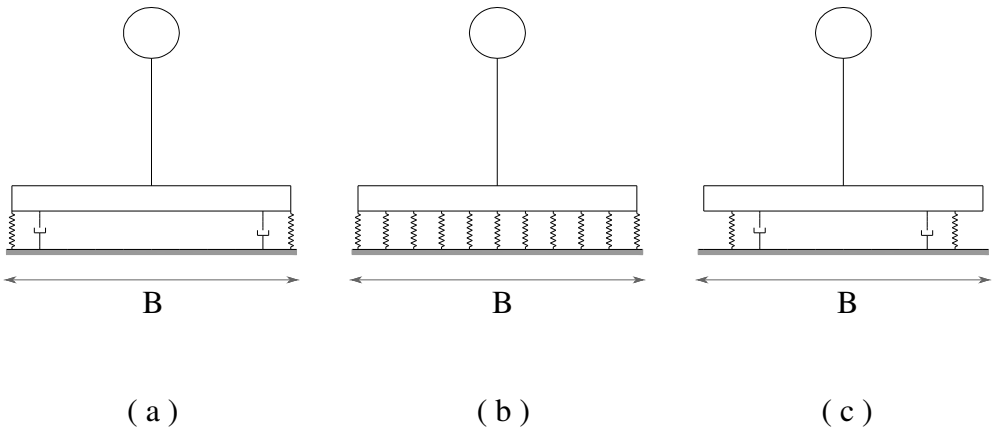


**Figure 1.2.** Simple models employed for response calculations during foundation uplift: (a) Two-spring model, (b) Winkler model, (c) S model.

Apart from the simplified models, the use of finite elements for modeling elastic continuum is a computationally expensive but accurate alternative (Wolf, 1976; McCallen and Romstad, 1994). A third approach to model uplifting of foundations is to use conical models in order to compute the stiffness of foundations and the dimensions of contact surface beneath the foundation (Wolf, 1976). The accuracy of the latter model is similar to that of finite element approach, although its computational cost is lower.

Several methods are employed for integration of equation of motion in order to compute the response of structures on uplifting foundations. Analytical solutions for differential equations can be directly employed for very simple problems that involve inversed pendulum structures resting on two-spring models (Song and Lee, 1992; Oliveto et al., 2002). Rayleigh-Ritz method or Galerkin's method can also be introduced in order to obtain approximate solutions for such simple models (Solomon et al., 1984; Celep and Güler, 1990).

However, when more complicated structural and foundation models should be introduced in analyses, numerical integration schemes such as Newmark's method (see Chopra, 2007, for complete description of the scheme) are useful. The variation in instantaneous stiffness of foundation should be computed by an external routine, which first estimates the dimensions of contact surface beneath the foundation due to instantaneous loads exerted on foundation. Applications with Newmark's scheme with Winkler and conical models are presented in literature (Wolf and Skrikerud, 1978; Wolf, 1976; and Mergos and Kavashima, 2005). Typical moment-rotation ($M$-$\theta$) response of a rectangular Winkler foundation to seismic loading is shown in Figure 1.3. On the other hand, Runge-Kutta method is a very accurate substitute for Newmark's scheme for solution of foundation uplift problems (Wang and Gould, 1993).

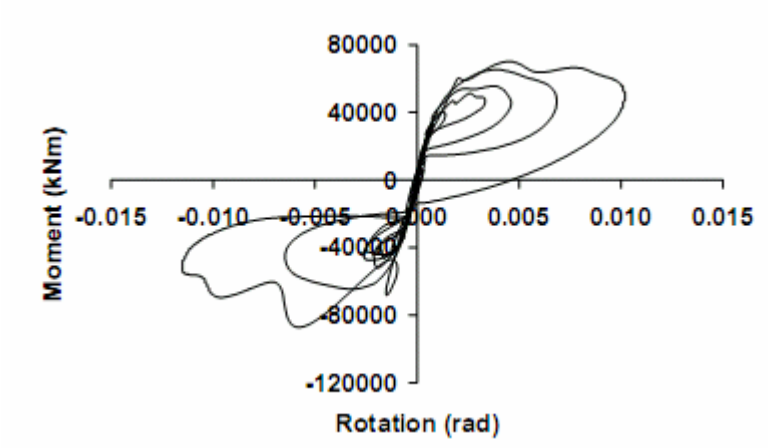


**Figure 1.3.** *M-θ* response of a typical bridge pier on Winkler foundation under severe seismic loading (Mergos and Kavashima, 2005)

## 1.3 Objectives of the Study

The primary objective of this study is to develop two algorithms, one to compute static uplift response of a shallow foundation resting on linear soil, and one to compute dynamic response of a single-degree-of-freedom (i.e., an inversed pendulum) structure during foundation uplift. Both algorithms call external routines for calculation of foundation stiffness (i.e., impedance) coefficients and dynamic algorithm also calls damping ones, so that any impedance formulae given for different soil behaviors and foundation geometries can be easily introduced. This is necessary in order to introduce models that consider nonlinear soil behavior, soil heterogeneity and foundation embedment, so that realistic calculation of foundation displacements under severe seismic loading can be possible. The second algorithm is based on Runge-Kutta method, therefore it is straightforward to employ available computing libraries for the solution of uplift problems. For simplicity, the horizontal displacement of foundation and the effect of out-of-plane loading on nonlinear response of foundation are omitted.

The secondary objective of this study is to criticize Winkler model, which is widely used in literature for the calculation of dynamic response of structures

during foundation uplift. Static moment-rotation ($M$-$\theta$) relationship of Winkler model is compared with that of a foundation on elastic half-space, through employing formulae for static stiffness of rectangular shallow foundations on elastic half-space. Hence, the significance of coupling between vertical displacement and rotation of foundations during uplift is critically evaluated.

There are four chapters in this thesis: Chapter 1 involves a brief literature survey on analysis of foundation uplift during seismic excitation, and the scope of this study. The algorithm developed to compute the static response of a shallow foundation, and the limitations of Winkler model are presented in Chapter 2. In Chapter 3, the second algorithm based on Runge-Kutta method is presented, which is used for computing the dynamic response of an inversed pendulum structure on Winkler foundation. The significance of vertical oscillations in rocking of structure-foundation system is also discussed in Chapter 3. Finally, Chapter 4 presents the summary of the study and its findings.

# CHAPTER 2

# STATIC RESPONSE OF UPLIFTING FOUNDATION

In order to assess the accuracy of Winkler model in simulation of foundation uplift on elastic half-space, the response of a foundation resting on Winkler support to static loading is compared with that on elastic half-space. The contact width of rectangular rigid foundation is computed for both support models consistently, as presented in the following. The resultant force acting on base of an uplifting foundation is calculated through employing the formulas given for the static stiffness of rectangular shallow foundation resting on elastic half-space. Hence, the calculation method is applicable for all foundation impedance formulas, irrespective of heterogeneity of supporting soil and foundation geometry. In this study, only in-plane loading is considered, so that rectangular foundation rotates only around its longitudinal axis. The methodology and the results of analyses are presented in the following.

## 2.1 Methodology

The numerical procedure for determination of static response of foundation permitted to uplift is presented in the following.

### 2.1.1 Static impedance of an uplifting foundation

Considering a rectangular shallow foundation of (in-plane) width $B$ and (out-of-plane) length $L$, the vertical displacement $v$ and rotation $\theta$ induced by vertical load $V$ and in-plane moment $M$ (Figure 2.1) are calculated by employing the following system of equations:

$$\begin{Bmatrix} V \\ M \end{Bmatrix} = \begin{bmatrix} K_v(B,L) & 0 \\ 0 & K_\theta(B,L) \end{bmatrix} \cdot \begin{Bmatrix} v \\ \theta \end{Bmatrix} \quad (2.1.a)$$

or,

$$\begin{Bmatrix} V \\ M \end{Bmatrix} = [K(B,L)] \cdot \begin{Bmatrix} v \\ \theta \end{Bmatrix} \quad (2.1.b)$$

where, $K_v$ and $K_\theta$ are the static impedance coefficients of shallow foundation, which are dependent on foundation dimensions as well as the stiffness of load bearing soil, and $[K(B,L)]$ is the stiffness matrix of rectangular foundation that is in full contact with the supporting soil. Sign conventions for $v$ and $\theta$ are the same as those given for $V$ and $M$ respectively (Figure 2.1).

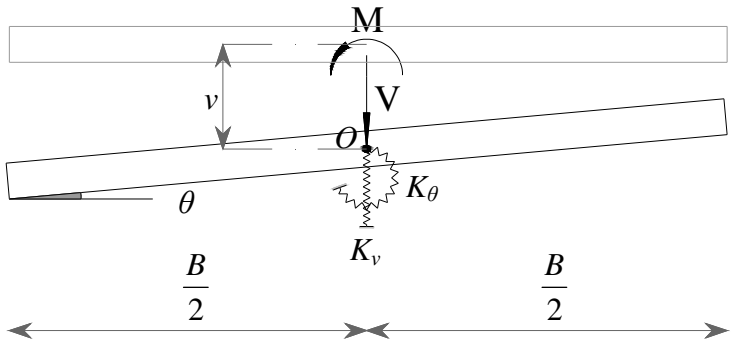


**Figure 2.1.** Sign convention for in-plane loads acting on a rigid rectangular foundation.

In case of foundation uplift, the section of rectangular foundation that is in contact with soil can be considered as a shallow rectangular foundation of width $B'$ (Figure 2.2). Therefore, substitution of $B'$ for $B$ in equation 2.1 results in static equilibrium equations for foundation during uplift:

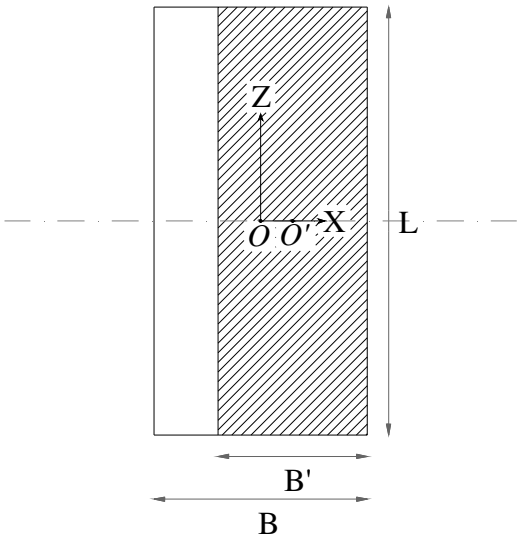


**Figure 2.2.** Reduction in effective foundation width ($B$) due to loss of contact with soil during uplift: shaded area is presumed to be in contact with soil.

$$\begin{Bmatrix} V' \\ M' \end{Bmatrix} = \begin{bmatrix} K_v(B',L) & 0 \\ 0 & K_\theta(B',L) \end{bmatrix} \cdot \begin{Bmatrix} v' \\ \theta' \end{Bmatrix} \qquad (2.2.a)$$

or,

$$\begin{Bmatrix} V' \\ M' \end{Bmatrix} = \left[K(B',L)\right] \cdot \begin{Bmatrix} v' \\ \theta' \end{Bmatrix} \qquad (2.2.b)$$

where, $V'$ and $M'$ are the vertical load and moment acting on the center of rectangular contact area, and $v'$ and $\theta'$ are the vertical displacement and rotation of the center of rectangular contact area (point $O'$ in Figure 2.2). The relationship between $\{v'\ \theta'\}^T$ and $\{v,\ \theta\}^T$ is given by (Figure 2.3).

$$\begin{Bmatrix} v' \\ \theta' \end{Bmatrix} = [A] \cdot \begin{Bmatrix} v \\ \theta \end{Bmatrix} \qquad (2.3)$$

where, assuming small deflections (i.e., $\tan(\theta) \cong \theta$),

$$[A]=\begin{bmatrix} 1 & sgn(\theta)\cdot\left(\dfrac{B-B'}{2}\right) \\ 0 & 1 \end{bmatrix} \qquad (2.4)$$

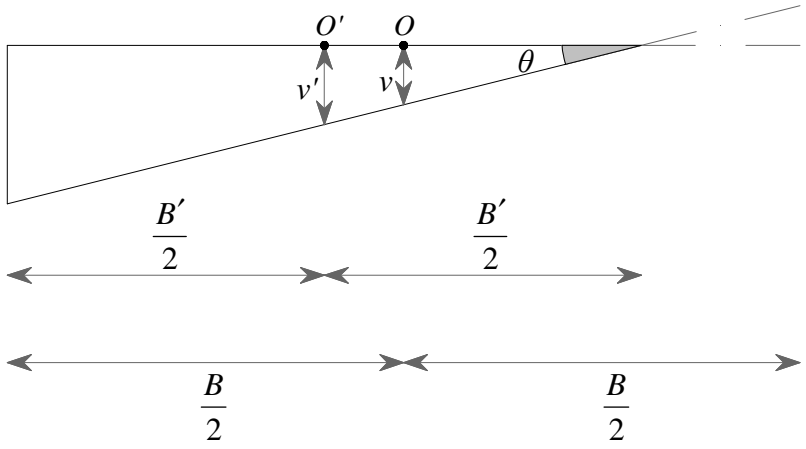


**Figure 2.3.** Determination of vertical displacement ($v'$) and rotational displacement ($\theta'$) at the midpoint of the contact area after uplift in terms of $v$ - $\theta$

Using general transformation rule (Cook et al., 1989), the relationship between resultant forces acting at the center of the foundation (pt. *O*) and the center of contact area (pt. *O´*) is

$$\begin{Bmatrix} V \\ M \end{Bmatrix} = [A]^T \cdot \begin{Bmatrix} V' \\ M' \end{Bmatrix} \qquad (2.5)$$

Substitution of equations 2.2.b and 2.3 in equation 2.5 results in the equation of static equilibrium for an uplifting foundation,

$$\begin{Bmatrix} V \\ M \end{Bmatrix} = [A]^T \cdot [K(B', L)] \cdot [A] \cdot \begin{Bmatrix} v \\ \theta \end{Bmatrix} \qquad (2.6.a)$$

or simply,

$$\begin{Bmatrix} V \\ M \end{Bmatrix} = \left[\overline{K}(B', L)\right] \cdot \begin{Bmatrix} v \\ \theta \end{Bmatrix} \qquad (2.6.b)$$

where $\left[\overline{K}(B', L)\right]$ is the static impedance matrix of an uplifting foundation. During uplift, the foundation impedance is dependent on the contact width $B'$ and foundation length $L$. On the other hand, $B'$ is dependent on foundation displacements, $v$ and $\theta$, hence (2.6) constitutes a nonlinear system of equations. The presumed relationship between the contact width and foundation displacements is presented in the following.

### 2.1.2 Estimation of contact width during uplift

The width of contact between a shallow foundation and soil during uplift can be computed by numerical models. The finite element method can be used to model the elastic half-space so that the contact width can be computed. An efficient approximate solution to the problem at hand is the use of cone models beneath the foundation and to introduce Green's function technique so that a computationally cheaper approach is obtained (Wolf, 1976). The Winkler model implicitly describes rules for calculation of contact width for a given vector $\{v\ \theta\}^{\mathrm{T}}$, presuming that the distributed springs beneath the foundation do not support tensile forces. The threshold overturning moment on foundation that initiates separation of shallow foundation from presumably elastic soil can be significantly different among different support models employed for uplift analyses.

Normalization of reaction forces is necessary before any comparison between different support models. Hence, $M$ can be normalized by $M_{ult}$, the ultimate (in-plane) overturning moment that can be exerted on a rectangular foundation:

$$M_{ult} = \frac{V \cdot B}{2} \qquad (2.7)$$

Considering a rigid foundation resting on deformable medium, it is presumed that the threshold moment for initiation of uplift, $M_{uplift}$, is proportional to $M_{ult}$, such that (Apostolou et al., 2006)

$$\left|M_{uplift}\right| = \alpha \cdot M_{ult} \qquad (2.8)$$

where, the dimensionless parameter $\alpha$ may depend on the shape of the foundation and mechanical properties of deformable half-space. Particular values for $\alpha$ are reported as 1/3 for circular foundations and 1/2 for strip foundations resting on elastic half-space (Wolf, 1976). $\alpha$ is 1/3 for a rectangular foundation on Winkler springs. Hence, in case of a strip foundation on Winkler springs, $M_{uplift}$ is significantly lower than that on elastic half-space. Therefore, in this study, the significance of parameter $\alpha$ in modeling uplift response of a shallow foundation will be examined through comparisons of foundation response to static loading when $\alpha$=1/3 and 1/2.

Foundation rotation and vertical displacement at the initiation of uplift is calculated through substitution of $M_{uplift}$ for $M$ in equation 2.1. Hence, Substitution of equations 2.7 and 2.8 in 2.1 results in

$$\left|\theta\right| = \alpha \cdot \frac{V \cdot B}{2 \cdot K_{\theta}(B,L)} \qquad (2.9.a)$$

or, the foundation begins to separate from supporting media when

$$0 = \frac{\alpha}{2} \cdot \frac{K_{v}(B,L) \cdot B^{2}}{K_{\theta}(B,L)} - \frac{B \cdot \left|\theta\right|}{v} \qquad (2.9.b)$$

Recalling that there are no coupling terms in $[K(B,L)]$ for degrees of freedom $v$ and $\theta$ (equation 2.1), the threshold $\theta$ for uplift is linearly related to $v$. However, when $\theta$ (or, $M$) exceeds the threshold for uplift, the contact width $B'$ should be

considered as the effective width of a shallow foundation. In that case, equation 2.9.b is not useful, since equation 2.1 is not valid. Thus, equation 2.2 should be used for calculation of $B'$. Instead, a simpler approach to the solution of problem at hand is to substitute $B'$, $v'$ and $\theta'$ in equation 2.9.b, for $B$, $v$ and $\theta$ respectively:

$$0 = \frac{\alpha}{2} \cdot \frac{K_v(B', L) \cdot (B')^2}{K_\theta(B', L)} - \frac{B' \cdot |\theta'|}{v'} \qquad (2.10)$$

Substitution of equation 2.3 in equation 2.10 results in

$$\frac{B' \cdot |\theta'|}{v + \cdot \left( \frac{B - B'}{2} \right) \cdot |\theta|} = \frac{\alpha}{2} \cdot \frac{K_v(B', L) \cdot (B')^2}{K_\theta(B', L)} \qquad (2.11.a)$$

or,

$$0 = \left( \frac{K_\theta(B', L)}{K_v(B', L) \cdot (B')^2} + \frac{\alpha}{4} \right) \cdot B' - \frac{\alpha}{2} \cdot \left( \frac{v}{|\theta|} + \frac{B}{2} \right) \qquad (2.11.b)$$

Hence, for a given vector $\{v'\ \theta'\}^T$, $B'$ can be calculated by finding the root of function given by equation 2.11. On the other hand, computation of $\{v\ \theta\}^T$ for a given load vector $\{V\ M\}^T$ requires solution of the nonlinear system of equations 2.6, since the terms in $\left[\overline{K}(B', L)\right]$ are dependent on $\{v\ \theta\}^T$. Iterative method to solve 2.6 is outlined in the following.

### 2.1.3 Iterative method for solution of static uplift problem

In order to compute the relationship between $M$ and $\theta$ for an uplifting foundation under static loading, the vertical load $V$ is kept constant, and the overturning moment $M$ acting on foundation is increased with small increments. Before the initiation of foundation uplift, the linear system of equations given as equation 2.1 is solved for computation of $\{v\ \theta\}^T$. In fact, since $v$ and $\theta$ are

uncoupled before uplift, it is necessary to compute only $\theta$ for a given $M$. The vertical displacement, $v$, is constant during the linear phase of static loading.

The foundation uplift will begin if $\theta$ exceeds the root of the function given as equation 2.9.b. In that case, equation 2.6.a should be used for determination of foundation response, whereas $B'$ should satisfy equation 2.11.b. Hence fixed-point iteration technique (Chapra and Canale, 2006) is employed, such that,

$$\begin{Bmatrix} V \\ M \end{Bmatrix} = \left[\overline{K}(B_i', L)\right] \cdot \begin{Bmatrix} v \\ \theta \end{Bmatrix}_{i+1} \qquad (2.12)$$

where, $B'_i$ is the contact width that corresponds to the i$^{th}$ solution vector $(\{v\ \theta\}^T)_i$ , and is computed by finding the root of equation 2.11.b. However, in order to overcome convergence problems that arise during iterations, underrelaxation technique is introduced in order to estimate $B'_i$, such that

$$(B_i')^{new} = \lambda \cdot B_i' + (1-\lambda) \cdot B_{i-1}' \qquad (2.13)$$

where, $(B_i')^{new}$ is used for computation of $(\{v\ \theta\}^T)_{i+1}$. It is observed that the choice of $\lambda$=0.5 is sufficient for convergence of iterations. Iterations are stopped when approximate relative percent error $(B_i')^{new}$ is less than 0.1%.

Matlab R13 is used as the computation environment. Hence, the function *fzero,* is used for finding the root of equation 2.11.b, with the constraint $0<B'<B$. *fzero* employs combinations of bisection, secant, and inverse quadratic interpolation methods for finding roots. Gauss-Elimination method implemented in Matlab is used for solving equations 2.1 and 2.12. Details of these methods are presented by Chopra (2007). The static impedance of rectangular shallow foundation is computed by employing the formulae given in the following sections.

## 2.2 Static impedance coefficients for a shallow foundation

In the following, the static impedance coefficients for a rectangular shallow foundation resting on Winkler springs and on elastic half-space are given. The width of the foundation is $B$ and length of foundation is $L$. The impedance coefficients during uplift, $K_\theta(B',L)$ and $K_v(B',L)$, can be calculated by substitution of $B'$ for $B$.

### 2.2.1 Foundation on Winkler springs

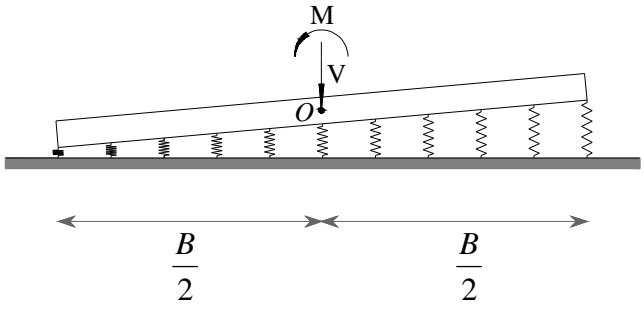


( a )

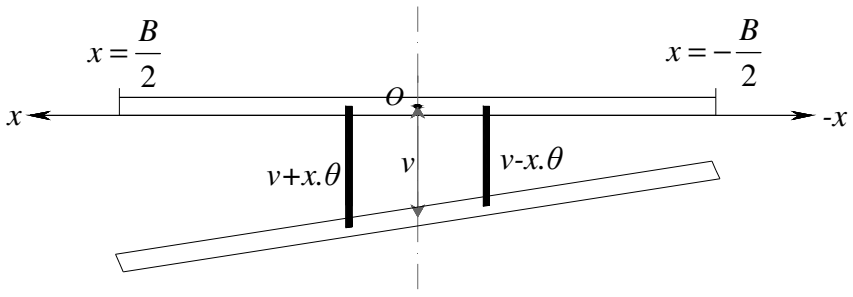


( b )

**Figure 2.4.** a) A rigid foundation resting on tensionless Winkler springs, b) Free body diagram for Winkler model.

Determination of static impedance of a rigid rectangular foundation resting on (distributed) Winkler springs with coefficient $k_0$ is straightforward (Figure 2.4). The moment equilibrium requires

$$M = L \cdot k_0 \cdot \left[ \int_0^{B/2} (v + x \cdot \theta) \cdot x \cdot \mathrm{d}x - \int_{-B/2}^{0} (v - x \cdot \theta) \cdot x \cdot \mathrm{d}x \right] \qquad (2.14.a)$$

or,

$$M = K_\theta(B, L) \cdot \theta \qquad (2.14.b)$$

where,

$$K_\theta(B, L) = \frac{1}{12} \cdot k_0 \cdot B^3 \cdot L \qquad (2.14.c)$$

is the rocking stiffness of Winkler foundation. Similarly, the load equilibrium requires

$$V = L \cdot k_0 \cdot \left[ \int_{-B/2}^{0} (v - x \cdot \theta) \cdot \mathrm{d}x + \int_0^{B/2} (v + x \cdot \theta) \cdot \mathrm{d}x \right] \qquad (2.15.a)$$

or,

$$V = K_V(B, L) \cdot v \qquad (2.15.b)$$

where,

$$K_v(B, L) = k_0 \cdot B \cdot L \qquad (2.15.c)$$

is the vertical stiffness of Winkler foundation.

### 2.2.2 Foundation on elastic halfspace

The response of an elastic halfspace bearing the dynamic loads acting on a foundation can be analyzed by employing rigorous analytical or numerical techniques. However, it is also possible to replace the halfspace beneath a foundation with simple discrete elements, such that the discrete elements

accurately simulate the actual response of an elastic halfspace. These discrete elements are generally composed of spring and dashpot elements with frequency dependent coefficients, namely the impedance coefficients (Figure 2.5). The static (i.e., zero-frequency excitation) impedance coefficients for a shallow foundation resting on homogeneous elastic half-space are presented by Gazetas (1991) as in the following:

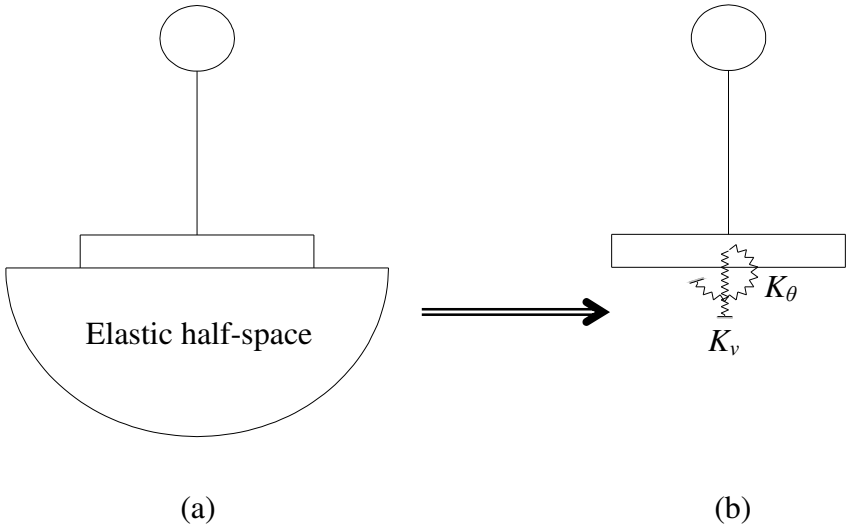


**Figure 2.5.** A shallow foundation (a) on elastic half-space, and (b) on discrete elements that simulate the response of elastic half-space.

For an arbitrarily shaped shallow foundation resting on surface of an elastic half-space, the rocking stiffness around longitudinal axis is

$$K_\theta = \frac{G}{1-\upsilon} I_{bx}^{0.75} \left(\frac{L}{B}\right)^{0.25} \left[2.4 + 0.5 \cdot \left(\frac{B}{L}\right)\right]$$

where $I_{bx}$ is the area moment of inertia of the foundation-soil contact around the longitudinal axis, $L$ is the length of foundation, $B$ is the width of foundation, $G$ and $\upsilon$ are respectively the shear modulus and Poisson's ratio of the homogeneous

elastic half-space that supports the foundation (Gazetas, 1991). Substitution of $I_{bx}=B^3 \cdot L/12$ for a rectangular foundation gives

$$K_\theta(B,L) = \frac{G}{1-\nu} \cdot \left( \frac{1}{12} \cdot B^3 \cdot L \right)^{0.75} \cdot \left( \frac{L}{B} \right)^{0.25} \cdot \left( 2.4 + 0.5 \cdot \frac{B}{L} \right) \qquad (2.16.a)$$

or,

$$K_\theta(B,L) = \frac{G \cdot B^2 \cdot L}{1-\nu} \cdot \left( 0.372 + 0.078 \cdot \frac{B}{L} \right) \qquad (2.16.b)$$

The static vertical stiffness of an arbitrarily shaped foundation is formulated by Gazetas (1991) as

$$K_v = \frac{2GL}{1-\upsilon} \left( 0.73 + 1.54 \chi^{0.75} \right)$$

where, $\chi = A_b / 4L^2$, and $A_b$ is the area of foundation-soil contact surface. Since $A_b=B \cdot L$ for a rectangular foundation on surface of an elastic half-space, the vertical stiffness of a rectangular shallow foundation is

$$K_v(B,L) = \frac{G \cdot L}{1-\nu} \cdot \left( 0.73 + 1.54 \cdot \left( \frac{B}{L} \right)^{0.75} \right) \qquad (2.17)$$

Presuming that the formulas given by Gazetas provide very accurate approximations of foundation stiffness on elastic half-space, the accuracy of Winkler model is examined through comparisons with the response of elastic halspace that is computed by employing equations 2.16 and 2.17.

### 2.3 An assessment of efficiency of Winkler springs in static uplift analysis

A comparison of equations 2.14 and 2.15 with 2.16 and 2.17 shows that the Winkler model cannot simulate the rocking and vertical impedance of a shallow

foundation simultaneously. For instance, in case of a square foundation ($B$=$L$), the impedance ratio $K_\theta/(K_v \cdot B^2)$ is 0.20 and 0.08 for a foundation resting on elastic half-space and Winkler springs, respectively. Since $\upsilon$ and $\theta$ are coupled during uplift, the consistence between two support models is questionable. Besides, the discrepancy between two models can significantly increase during uplift, since $K_\theta$ is proportional to $(B')^3$ for Winkler model, but approximately proportional to $(B')^2$ for elastic half-space. In the following, the rocking stiffness of a square foundation resting on Winkler support is compared with that on elastic half-space.

### 2.3.1 Comparison of $M$-$\theta$ relationship for two support models

In order to compare the static moment-rotation ($M$-$\theta$) relationship for a foundation resting on elastic half-space and that supported by Winkler springs, the vertical load is kept constant (i.e., $V$=$mg$, where m is the mass of structure) and overturning moment acting on foundation ($M$) is increased incrementally. It is presumed that, $M_{uplift}$ is the same for both models. Hence, two sets of analysis with $\alpha$=1/3 and $\alpha$=1/2 are performed. A square foundation is considered in analyses. Remaining parameters employed in analyses are presented in Table 2.1. The coefficient of Winkler springs ($k_0$) is calculated assuming either that the rocking impedance coefficients determined for Winkler and elastic half-space models are consistent, or that the vertical impedance coefficients are consistent. Hence, for the first case, $k_{0\theta}$ is computed assuming that equation 2.14 is equivalent to 2.16. For the second case, $k_{0v}$ is computed assuming that equations 2.15 and 2.17 are equivalent.

**Table 2.1.** Parameters employed in analyses to determine $M$-$\theta$ relationships.

| $m$ (mass) (ton) | $B$ (m) | $L$ (m) | $h$ (height) (m) | $G$ (kN / m$^2$) | $\nu$ |
|---|---|---|---|---|---|
| 1000 | 10 | 10 | 20 | 100000 | 0.3 |

The results of analyses are presented in Figure 2.5. The moment $M$ is normalized by $VB$, and rotations are normalized by $VB/K_\theta\,(B,L)$, where $K_\theta\,(B,L)$ is computed by equation 2.16.b (i.e., impedance of foundation on elastic half-space). Hence, for a foundation resting on elastic half-space, or that on Winkler springs with $k_0 = k_{0\theta}$, the threshold normalized foundation rotation at the initiation of uplift is equal to $\alpha/2$.

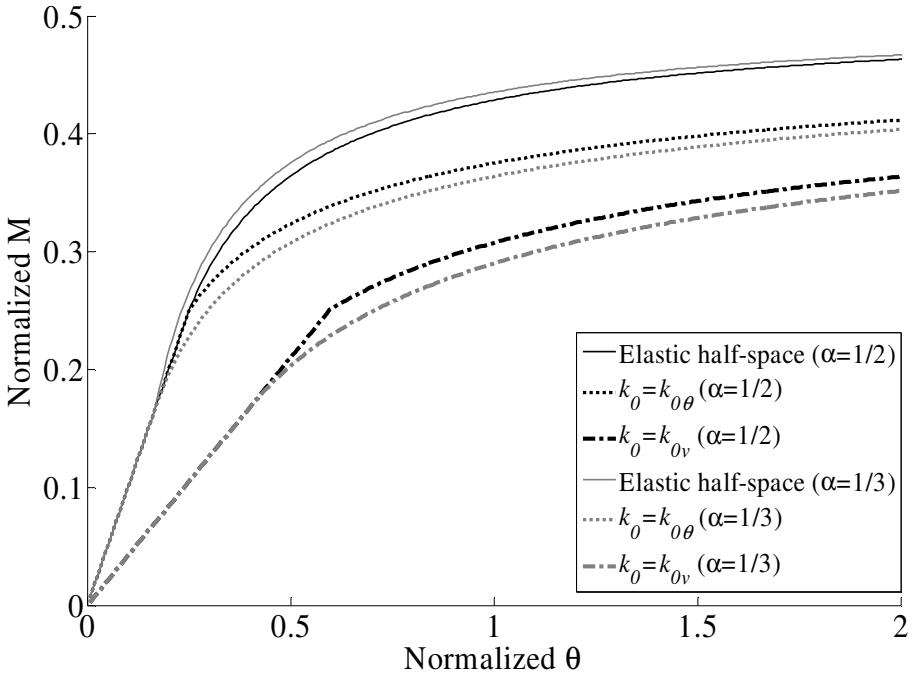


**Figure 2.6.** $M - \theta$ relationship for a square foundation under static loading.

The results given in Figure 2.6 show that $M$-$\theta$ relationship for a foundation on elastic support is similar for the cases $\alpha$=1/2 and $\alpha$=1/3. Unless experimental findings for rectangular foundations on real soils, which behave nonlinearly, show dissimilar values for $\alpha$, the choice $\alpha$=1/3 for a foundation presumably resting on elastic half-space is appropriate for engineering purposes. Hence, the assumption that $\alpha$=1/3, which is implicit in Winkler model, does not result in significant error in uplift calculations. However, $M$-$\theta$ relationships for Winkler model and for elastic half-space models are remarkably different.

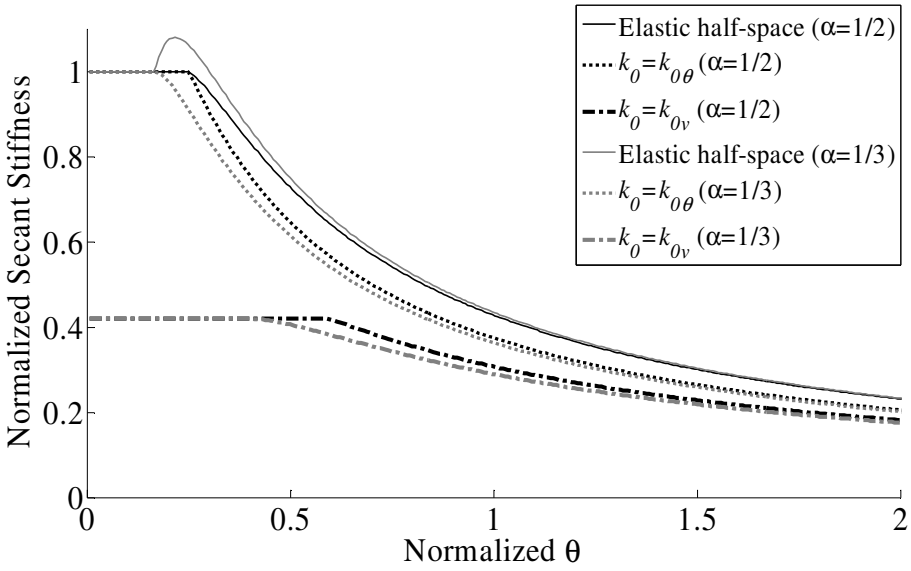


**Figure 2.7.** Normalized secant rotational stiffness of a square foundation under static loading**.**

The significance of the differences between two models is further investigated by computing the variation of secant rotational stiffness ($M/\theta$) by $\theta$. The secant stiffness is the apparent stiffness of foundation under static loading, and during steady-state response under harmonic loading, since it is a function of maximum $\theta$. The secant stiffness is normalized by the initial rotational stiffness (i.e., $K_\theta(B,L)$) of elastic half-space model (Figure 2.7). It is observed that the secant rotational stiffness of foundation on Winkler springs is converging to that of foundation on elastic half-space by increasing $\theta$, irrespective of the choice for $k_{0.}$ The rotational impedance of a shallow foundation resting on Winkler model and that on elastic half-space is similar, in case $k_{0\theta}$ is employed in analyses.

When $\alpha$=1/3 is assumed for elastic half-space model, a small increase in secant rotational stiffness is observed at lower range of $\theta$. For, $\alpha$=1/2 no such an artificial increase is observed. Therefore, $\alpha$=1/3 is apparently lower than its real value. Although it is possible to obtain a rigorous formula for $\alpha$ such that $\alpha$ does not induce an artificial increase in rocking stiffness during the early stages of uplift, the practical significance of this issue is limited, because the maximum

value attained by normalized secant modulus is 1.08 in Figure 2.7, which implies that the relative percent error is less than 8% for a given $\theta$ and rapidly diminishes by increasing $\theta$. Such a small magnitude of error will induce a negligible effect on the dynamic response of a structure, since the period of an oscillator is inversely proportional to square root of its stiffness.

$k_0$=$k_{0v}$ is not a proper choice for foundation uplift analysis, since the initial rotational stiffness is much lower than the actual value for a foundation on elastic half-space. The discrepancy between $M$-$\theta$ curves of Winkler model and elastic half-space model is also significant for larger values of $\theta$. Hence, it is apparent that the main limitation of the Winkler model is that, it cannot simulate the vertical displacements (i.e., settlement) and rotations of a foundation simultaneously.

The relative percent error in secant rocking stiffness of a Winkler foundation is presented in Figure 2.8. It is assumed that equations 2.16 and 2.17 provide accurate estimates of impedance of a foundation on elastic half-space. Consistent values of $\alpha$ are chosen for Winkler and elastic half-space models so that the calculated error is free of the assumption made for $M_{uplift}$. It is observed that, the relative percent error for secant rocking stiffness ($M/\theta$) is less than 20% in case $k_0$=$k_{0\theta}$ is assumed for analysis. The error decreases by increasing $\alpha$.

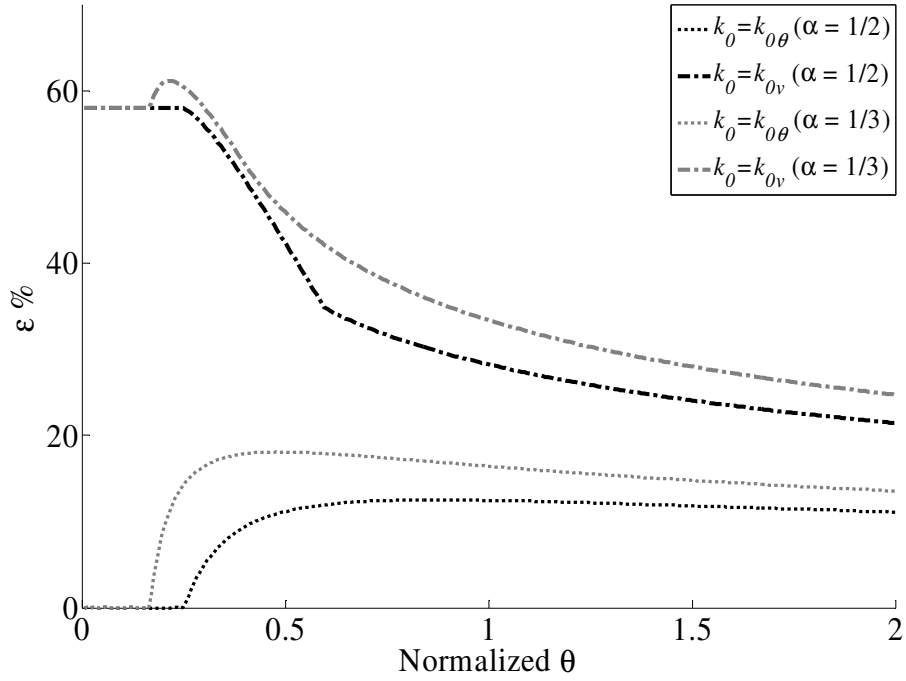


**Figure 2.8.** The relative percent error of secant rotational of a foundation on Winkler springs.

Finally, the significance of foundation geometry in determination of *M-θ* curve for a foundation is investigated, since the preceding results are obtained by computing the response of a square foundation (*L/B*=1). On the other hand, equations 2.16 and 2.17 involve the term *B/L*, showing the dependency of foundation impedance on its geometry. Although the Winkler model provides foundation impedance coefficients that are proportional to *L* (equations 2.14 and 2.15), the coefficients for a foundation on elastic half-space are nonlinearly related to *L*. The normalized *M-θ* relationship for a rectangular foundation (*L/B*=3) is compared with that for a square foundation (*L/B*=1) in Figure 2.9. It is observed that the effect of foundation geometry on normalized *M-θ* relationship is negligible. Hence, although the ratio *L/B'* increases by *θ* during uplift, the change in the geometry of foundation (i.e., contact surface) does not result in an additional source of deviation between Winkler and elastic half-space models. The results obtained for a square foundation are also representative for rectangular foundations.

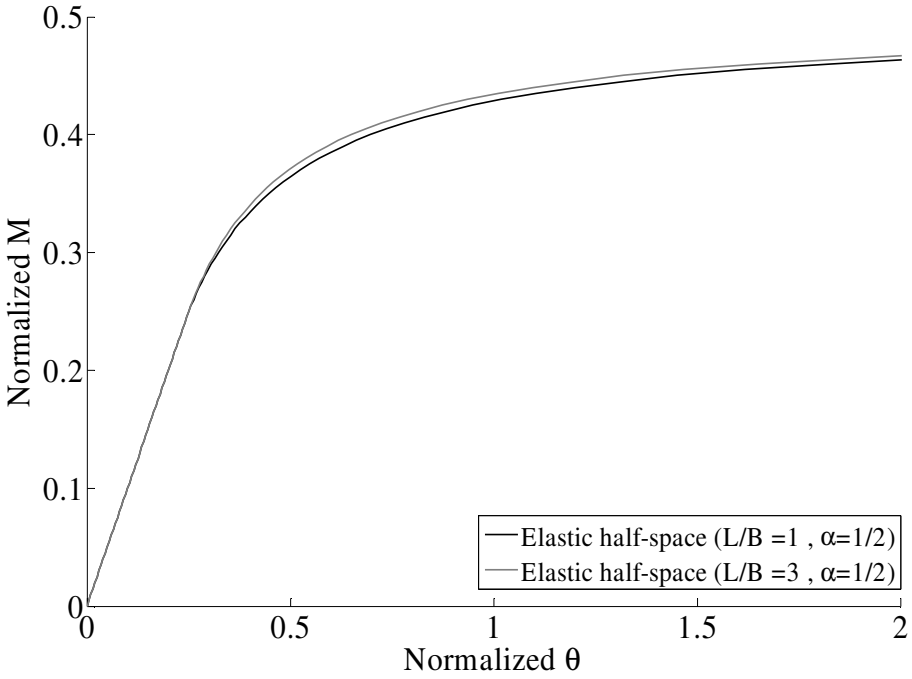


**Figure 2.9.** Comparison of normalized $M$-$\theta$ relationships for a rectangular ($L/B$=3) and a square foundation ($L/B$=1).

### 2.3.2 Comparison of $v$-$\theta$ relationship for two support models

It is apparent that the only limitation of Winkler model in uplift analysis is that it cannot predict the vertical and rotational response of a foundation simultaneously. This is also shown by comparing $v$-$\theta$ relationships of Winkler and elastic half-space models in Figure 2.10. When it is presumed that $k_0 = k_{0v}$, the vertical displacement of a Winkler foundation during uplift is significantly different from that of a foundation on elastic half-space. On the other hand, when it is presumed that $k_0 = k_{0\theta}$, the agreement between $v$-$\theta$ curves for Winkler and elastic half-space models is very limited, and the discrepancy between two models is very large in the early stages of loading.

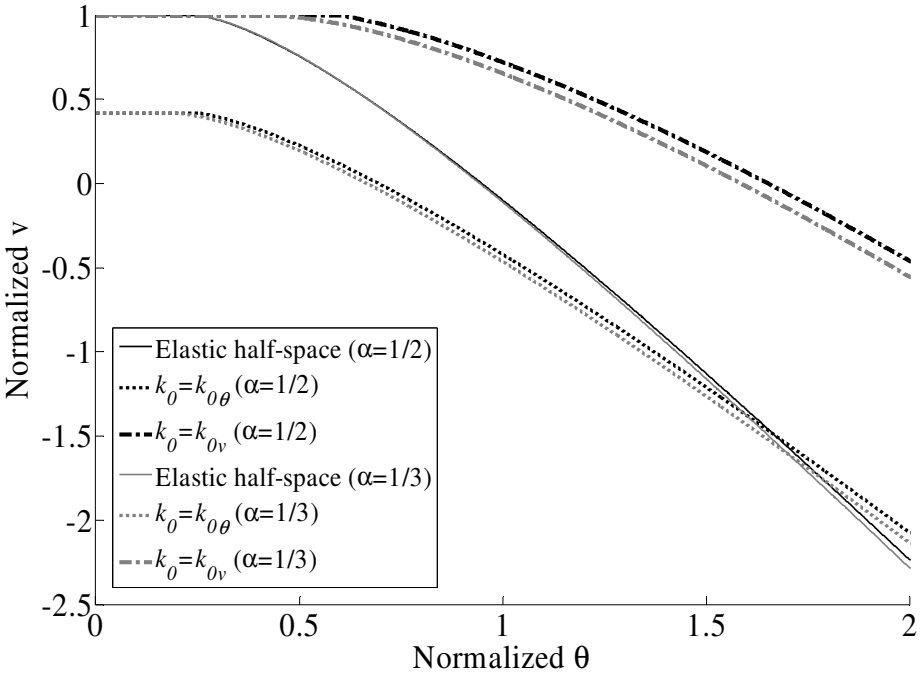


**Figure 2.10.** $v - \theta$ relationship for a square foundation under static loading.

# CHAPTER 3

# CALCULATION OF DYNAMIC RESPONSE DURING UPLIFT

## 3.1. Introduction

In this chapter, an algorithm to compute the dynamic response of an inversed pendulum (i.e., a single-degree-of-freedom) structure resting on an uplifting foundation is developed. The algorithm uses Runge-Kutta (RK) method for numerical solution of system of ordinary differential equations. The horizontal reaction force acting on foundation is omitted. Energy dissipation on foundation-soil interface through wave emission to deeper soils is simulated by viscous dampers (i.e., dashpots). Considering dashpot elements connected to pt $O$ (center of rigid foundation) parallel to springs with coefficients $K_v$ and $K_\theta$ in Figure 2.1, the damping coefficients are $C_v$ and $C_\theta$ for vertical oscillation and rocking motion respectively. A simple inversed pendulum structure on foundation is considered in analyses, which has only one structural degree of freedom. The structural stiffness and damping coefficients are $K_s$ and $C_s$ respectively. The mass of the structure, $m$, is lumped at height $h$ from the foundation (Figure 3.1).

First, the expressions for first derivatives of variables to be introduced in the RK algorithm are derived by employing the dynamic equilibrium equations for the system shown in Figure 3.1. Then, solution for a given set of parameters is obtained by calling the function ODE23 in Matlab, which employs a second and a third order RK method to obtain numerical solutions to ordinary differential equations. The $M$-$\theta$ relationship computed by the RK method is compared with that obtained by the iterative procedure given for static loading in Chapter 2. Only horizontal excitation of structure is considered. Foundation impedance coefficients, $K_v$, $K_\theta$, $C_v$, and $C_\theta$, are computed by employing Winkler model that

involves distributed dashpot elements with coefficient $c_0$.

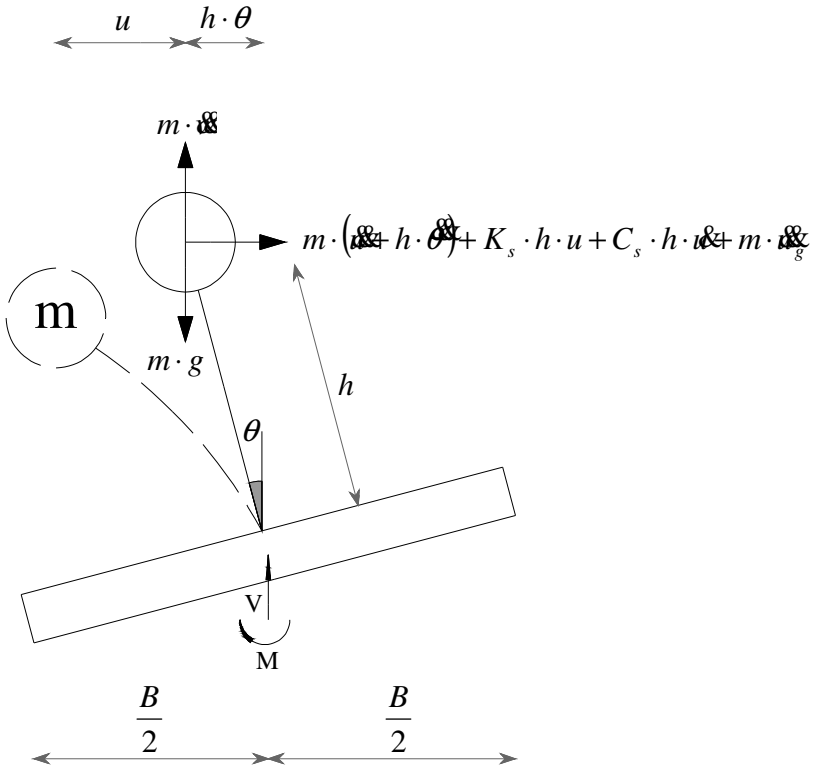


**Figure 3.1.** The forces acting on an inversed pendulum structure on rectangular foundation.

### 3.2 Methodology

The damping force should be added to equation 2.1 in order to obtain equilibrium equations for a shallow foundation under dynamic loading

$$\begin{Bmatrix} V \\ M \end{Bmatrix} = \begin{bmatrix} K_v(B,L) & 0 \\ 0 & K_\theta(B,L) \end{bmatrix} \cdot \begin{Bmatrix} v \\ \theta \end{Bmatrix} + \begin{bmatrix} C_v(B,L) & 0 \\ 0 & C_\theta(B,L) \end{bmatrix} \cdot \begin{Bmatrix} \dot{v} \\ \dot{\theta} \end{Bmatrix} \qquad (3.1.a)$$

or,

$$\begin{Bmatrix} V \\ M \end{Bmatrix} = [K(B,L)] \cdot \begin{Bmatrix} v \\ \theta \end{Bmatrix} + [C(B,L)] \cdot \begin{Bmatrix} \dot{v} \\ \dot{\theta} \end{Bmatrix} \quad (3.1.b)$$

where, $C_v$ and $C_\theta$ are the coefficients of dashpots that react vertical and angular velocity of foundation. The number of dots on a variable represents the order of derivative with respect to time. Following the steps presented in section 2.1, the equilibrium equations after initiation of uplift are

$$\begin{Bmatrix} V' \\ M' \end{Bmatrix} = \begin{bmatrix} K_v(B',L) & 0 \\ 0 & K_\theta(B',L) \end{bmatrix} \cdot \begin{Bmatrix} v' \\ \theta' \end{Bmatrix} + \begin{bmatrix} C_v(B',L) & 0 \\ 0 & C_\theta(B',L) \end{bmatrix} \cdot \begin{Bmatrix} \dot{v} \\ \dot{\theta} \end{Bmatrix} \quad (3.2.a)$$

or,

$$\begin{Bmatrix} V' \\ M' \end{Bmatrix} = [K(B',L)] \cdot \begin{Bmatrix} v' \\ \theta' \end{Bmatrix} + [C(B',L)] \cdot \begin{Bmatrix} \dot{v} \\ \dot{\theta} \end{Bmatrix} \quad (3.2.b)$$

where $B'$ is width of contact area between foundation and soil. Substitution of equations 3.2.b and 2.3 in equation 3.1 results in the following system of equations:

$$\begin{Bmatrix} V \\ M \end{Bmatrix} = [A]^T \cdot [K(B',L)] \cdot [A] \cdot \begin{Bmatrix} v \\ \theta \end{Bmatrix} + [A]^T \cdot [C(B',L)] \cdot [A] \cdot \begin{Bmatrix} \dot{v} \\ \dot{\theta} \end{Bmatrix} \quad (3.3.a)$$

or,

$$\begin{Bmatrix} V \\ M \end{Bmatrix} = [\overline{K}(B',L)] \cdot \begin{Bmatrix} v \\ \theta \end{Bmatrix} + [\overline{C}(B',L)] \cdot \begin{Bmatrix} \dot{v} \\ \dot{\theta} \end{Bmatrix} \quad (3.3.b)$$

The vertical force ($V$) and overturning moment ($M$) exerted on foundation by inversed pendulum structure are given as

$$V = m \cdot g - m \cdot \ddot{v} \quad (3.4.a)$$

since inversed pendulum structure is presumed to be axially rigid, and

$$M = K_s \cdot h \cdot u + C_s \cdot h \cdot \dot{u} \qquad (3.4.b)$$

where, $m$ is the mass of structure lumped at height $h$ from foundation, $K_s$ and $C_s$ are the stiffness and damping coefficients of the inversed pendulum structure, respectively, and $u$ is the structural distortion (Figure 3.1). The relationship between total horizontal displacement of lumped mass ($u_t$), structural distortion ($u$), and rocking of foundation ($\theta$) is

$$u_t = u + h \cdot \theta \qquad (3.5)$$

Substitution of equation 3.5 in 3.4.b gives

$$M = K_s \cdot u_t \cdot h + C_s \cdot \dot{u}_t \cdot h - K_s \cdot h^2 \cdot \theta - C_s \cdot h^2 \cdot \dot{\theta} \qquad (3.6)$$

Then, substitution of equations 3.6 and 3.4.a in 3.3.b results in the following

$$\begin{Bmatrix} -m\ddot{u}_t \\ 0 \end{Bmatrix} - [D] \cdot \begin{Bmatrix} v \\ \theta \end{Bmatrix} = \{P\} \qquad (3.7.a)$$

where,

$$[D] = [\overline{C}(B', L)] + \begin{bmatrix} 0 & 0 \\ 0 & C_s h^2 \end{bmatrix} \qquad (3.7.b)$$

and

$$\{P\} = \left( [\overline{K}(B', L)] + \begin{bmatrix} 0 & 0 \\ 0 & K_s h^2 \end{bmatrix} \right) \cdot \begin{Bmatrix} v \\ \theta \end{Bmatrix} - \begin{Bmatrix} mg \\ K_s h u_t + C_s h \dot{u}_t \end{Bmatrix} \qquad (3.7.c)$$

Equation 3.7.a is employed for formulation of $\ddot{\theta}$ and $\ddot{u}$, such that

$$\ddot{\theta} = \frac{P_2 + D_{21} \cdot \ddot{v}}{-D_{22}} \qquad (3.8)$$

$$\ddot{u}_t = \frac{P_1 + D_{11} \cdot \ddot{v} + D_{12} \cdot \ddot{\theta}}{-m} \qquad (3.9)$$

where $D_{ij}$ represents the element of [$D$] located on the i$^{th}$ row and j$^{th}$ column, and $P_i$ represents the i$^{th}$ element of {P}. Hence, in order to compute $\ddot{\theta}$ and $\ddot{u}_t$, variables $u_t$ and $\dot{u}_t$ should be known at any calculation step. The numerical solutions for the latter variables are obtained by employing RK method: The horizontal equilibrium of forces acting on mass $m$ (Figure 3.1) requires that

$$m \cdot \ddot{u}_t + C_s \cdot \dot{u} + K_s \cdot u = -m \cdot \ddot{u}_g \qquad (3.10)$$

where, $\ddot{u}_g$ is the horizontal ground acceleration. Hence, substitution of equation 3.5 in 3.10 results in

$$\ddot{u}_t = -\frac{K_s}{m} \cdot u_t - \frac{C_s}{m} \cdot \dot{u}_t + \frac{K_s \cdot h}{m} \cdot \theta + \frac{C_s \cdot h}{m} \cdot \dot{\theta} - \ddot{u}_g \qquad (3.11)$$

Hence, the system of ordinary differential equations can be written as follows:

Integration of 3.11 by RK algorithm provides solution for $\dot{u}_t$. It is obvious that, calculation of $\ddot{\theta}$ by equation 3.8 should precede the use of equation 3.11.

In summary, equations 3.8, 3.9, and 3.11 are used for calculation of first derivatives of $\theta$, $\dot{v}$, and $\dot{u}_t$. In turn, $\dot{v}$ and $\dot{u}_t$ are integrated in order to compute $v$ and $u_t$. The structural distortion, $u$, is computed employing equation 3.5. Hence, the variables for which time-histories are computed are given in the vector $\{u_t \quad v \quad \theta \quad \dot{u}_t \quad \dot{v} \quad \dot{\theta}\}^T$. The vector of first derivatives of the variables is

given as $\{\dot{u}_t \quad \dot{v} \quad \dot{\theta} \quad \dot{u}_f \quad \dot{v}_f\}^T$. Assuming that the structure is at rest prior to horizontal excitation, the initial conditions are given as

$$\{u_t \quad v \quad \theta \quad u_f \quad v_f\}_0^T = \left\{0 \quad \frac{m \cdot g}{K_v(B,L)} \quad 0 \quad 0 \quad 0\right\}_0^T \qquad (3.12)$$

The initial condition for $v$ is equal to the static settlement of foundation under weight of structure.

Winkler model is used for computations. The static impedance coefficients ($K_\theta$ and $K_v$) are computed by employing equations 2.14 and 2.15. Similar to the expressions for $K_\theta$ and $K_v$, it is straightforward to show that

$$C_\theta(B,L) = \frac{1}{12} \cdot c_0 \cdot B^3 \cdot L \qquad (3.13)$$

and,

$$C_v(B,L) = c_0 \cdot B \cdot L \qquad (3.14)$$

Where, $c_0$ is damping coefficients for Winkler springs.

Uplift initiates when equation 2.9 is satisfied. Hence, for the calculation of contact width, it is assumed that the stress distribution beneath the foundation under dynamic loading is the same as the distribution under static loading for a given foundation displacement vector $\{v \quad \theta\}^T$. The limitations of the approximation of contact width, which is proposed by Wolf (1976), are investigated in the following section. Therefore, the contact width should be computed by finding the root of equation 2.11. In fact, considering tensionless Winkler springs beneath foundation (i.e., $\alpha$=1/3), equation 2.11 reduces to

$$B' = \frac{v}{|\theta|} + \frac{B}{2} \qquad (3.15)$$

At the initiation of uplift, $B'=B$, after substitution of equations 2.14 and 2.15, equation 2.9 (or, 3.15) reduces to

$$0 = \frac{v}{|\theta|} - \frac{B}{2} \qquad (3.16)$$

In literature, the above expression for the threshold rotation of a foundation uplift is also derived, by formulating the rotation necessary for inducing tensile forces on the leftmost (or, rightmost) Winkler spring (Psycharis, 2007). In dynamic response calculations, presented in the following section, equations 3.15 and 3.16 are used for calculation of contact width of foundation.

### 3.3 Parametric Analyses

In this section, parametric analyses are performed in order to investigate the efficiency of the algorithm in calculation of structural response when significant uplifting of foundation occurs. The parameters pertinent to stiffness and damping properties of the system shown in Figure 3.1 are given on Table 3.1.

**Table 3.1.** Parameters employed in dynamic analyses.

| $m$ (ton) | $B$ (m) | $L$ (m) | $h$ (m) | $k_0$ (kN/m$^3$) | $c_0$ (kN·s/m$^3$) | $K_s$ (kN/m) | $C_s$ (kN·s/m) |
|---|---|---|---|---|---|---|---|
| 1000 | 10 | 10 | 20 | 77100 | 247 | 195000 | 1396 |

Here, the mass $m$, foundation width $B$, foundation length $L$, and the height of the structure $h$ are arbitrarily selected. Hence, the period and damping ratio of inversed pendulum structure are $2\pi \cdot \sqrt{m/K_s} = 0.45$ s and $C_s \big/ 2\sqrt{K_s \cdot m} = 5$ %

respectively. By employing equations 2.14 and 2.15, the impedance coefficients are calculated to be $K_\theta = 6.430 \cdot 10^7$ kN·m/rad and $K_v = 7.71 \cdot 10^6$ kN/m. When horizontal deformation of foundation is omitted, natural period of structure on flexible foundation, $\overline{T}$, is calculated as 0.67 s through employing (Yılmaz, 2004):

$$\overline{T}^2 = T_s^{\,2} + T_\theta^{\,2} \qquad (3.17)$$

where,

$$T_\theta = 2 \cdot \pi \cdot \sqrt{\frac{m \cdot h^2}{K_\theta(B,L)}} \qquad (3.18)$$

is the natural period of a rigid inversed pendulum structure on flexible foundation. Employing equations 3.13 and 3.14, damping coefficients of foundation are calculated as $C_\theta = 2.06 \cdot 10^5$ kN·m·s/rad and $C_v = 2.47 \cdot 10^4$ kN·s/m. Hence, considering resonant response, the damping ratio for foundation impedance is calculated as $\pi \cdot \frac{c_0}{\overline{T} \cdot k_0} =$ 1.5 %.

A simple sinusoidal horizontal excitation is employed in analyses. Acceleration history of the ground motion is defined as

$$\ddot{u}_g = A \cdot \sin\left(\frac{2 \cdot \pi}{T_{exc}} \cdot t\right) \cdot \sin\left(\frac{2 \cdot \pi}{10 \cdot T_{exc}} \cdot t\right) \qquad (3.19)$$

where, $A$ is the amplitude and $T_{exc}$ is the excitation period. A long and a short period excitation is employed in analyses by setting $T_{exc} = 1.5 \cdot \overline{T}$ and $T_{exc} = 0.3 \cdot \overline{T}$, respectively.

### 3.3.1 Response to Long Period Excitation

The accuracy of analysis procedure is first investigated by considering response of inversed pendulum structure to a long period excitation, such that $T_{exc}=1.5\cdot\overline{T}$ and $A$=0.79 m/s$^2$. In Figure 3.2, normalized $M$-$\theta$ relationship is compared with that obtained for static loading of Winkler model (Figure 2.5). It is observed that, when equation 2.6 is employed so that viscous reaction forces are omitted in calculation of $M$, the $M$-$\theta$ relationship follows the static curve closely (Figure 3.2.a). When equation 3.1 is employed, viscous reaction forces are included in calculation of $M$, hysteretic loops around the static $M$-$\theta$ relationship are observed (Figure 3.2.b). Since $T_{exc}$ is relatively long, the viscous terms do not play a significant role in foundation reaction, and the reaction forces are almost equal to their static counterparts for all practical values of $\theta$ .

In Figure 3.3 the time-histories of $u_t$, $h\cdot\theta$, and $u$ are compared. Smooth sinusoidal variations of the response variables by time points out that, the contribution of $u$ and $h\cdot\theta$ in $u_t$ are similar in early stages of oscillations where reaction of foundation is linear, but the proportion of $h\cdot\theta$ in $u_t$ significantly exceeds that of $u$ when nonlinear response of foundation is more pronounced. Hence, considering the dynamic response of a slender structure on tensionless foundation, one can calculate that an increase in $u_t$ may not imply a similar increase in $u$.

When larger values of $A$ are selected, so that nonlinear response of foundation becomes more pronounced, excessive deviations from static $M$-$\theta$ curve are observed when $\theta$ attains its maximum. Similar results are obtained when higher order RK algorithms are also employed. One possible explanation is that, the omission of viscous reaction forces in calculation of $B'$ renders incorrect calculation of foundation impedance during uplift. The second possible explanation is that, vertical displacement ($v$) plays a significant role in foundation rocking during uplift. In order to understand the source of deviations from static $M$-$\theta$ relationship, the response of foundation to short period excitation is computed and presented in the following.

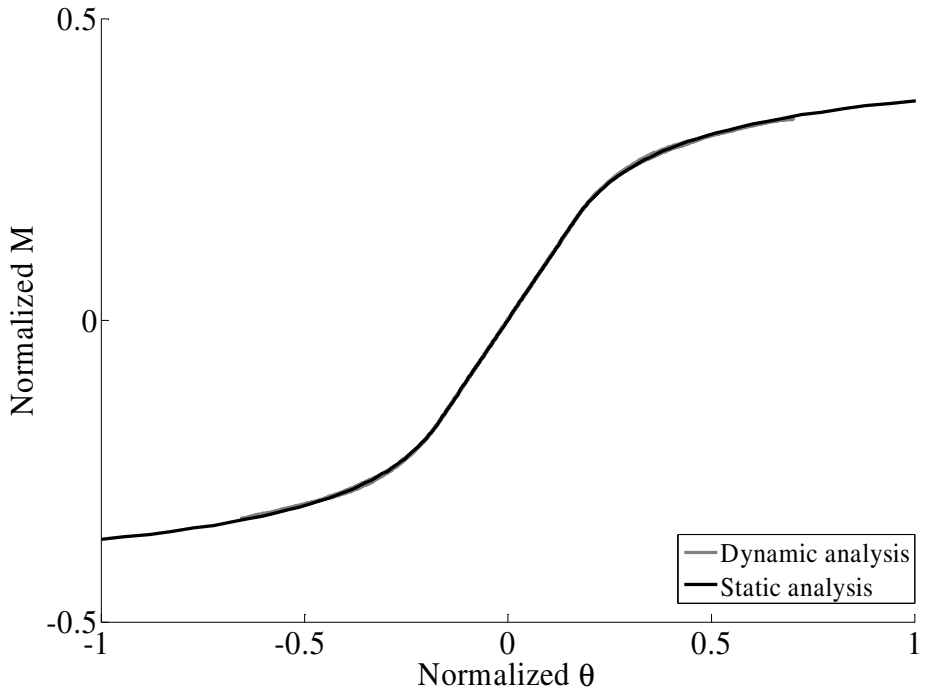


( a )

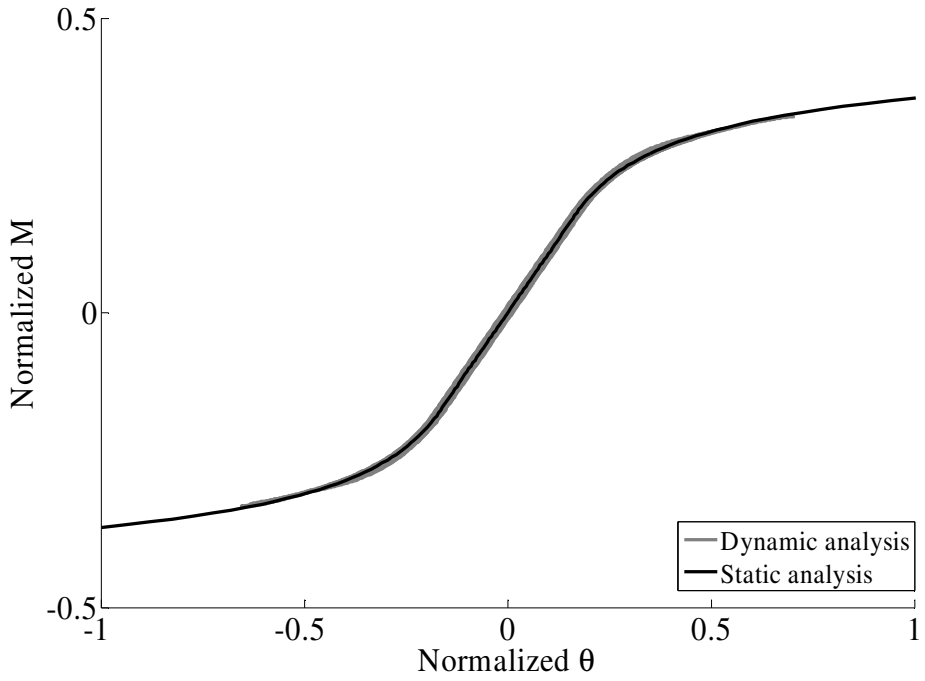


( b )

**Figure 3.2.** Comparison of *M-θ* response in dynamic analysis with that in static analysis for long period excitation by (a) employing equation 2.6, (b) employing equation 3.1.

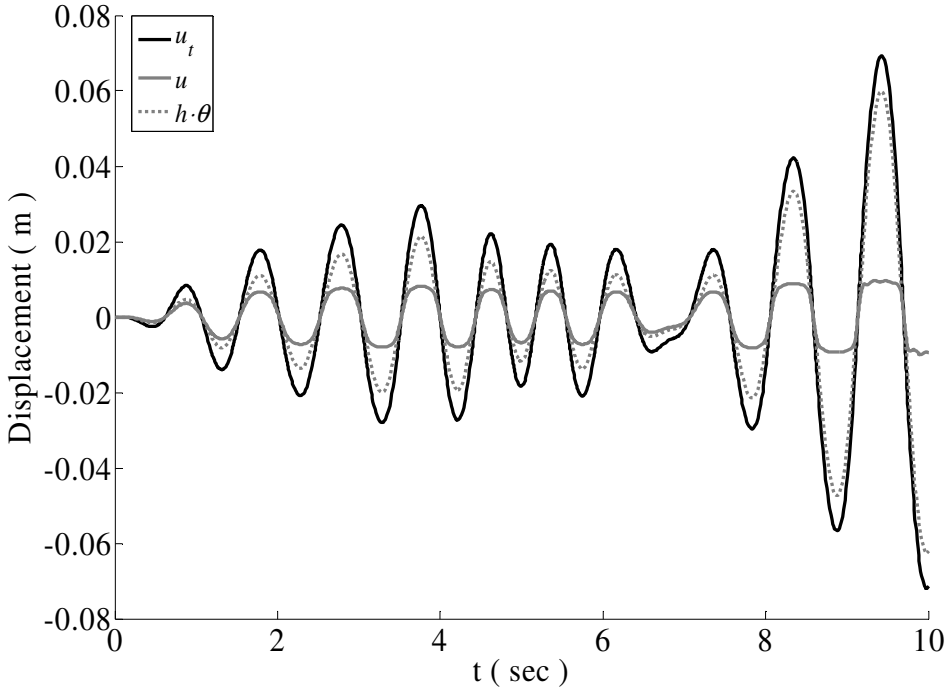


**Figure 3.3.** Comparison of $u_t$, $u$ and $h\cdot\theta$ histories for long period excitation.

### 3.3.2 Response to Short Period Excitation

In Figure 3.4, the computed response of foundation to short period excitation during uplift is compared with its static response presented in Chapter 2. The dynamic excitation parameters are chosen as $T_{exc} = 0.3 \cdot \overline{T}$ and $A$=20 m/s$^2$. Viscous response forces are more significant than those for long period excitation. Hence, wider hysteretic loops around static $M$-$\theta$ curve are observed in Figure 3.4.b. When equation 2.6 is used for calculation of $M$-$\theta$ relationship, significant deviations from the static backbone curve is observed in Figure 3.4.a. The source of deviations from static loading $M$-$\theta$ curve is discussed in the following.

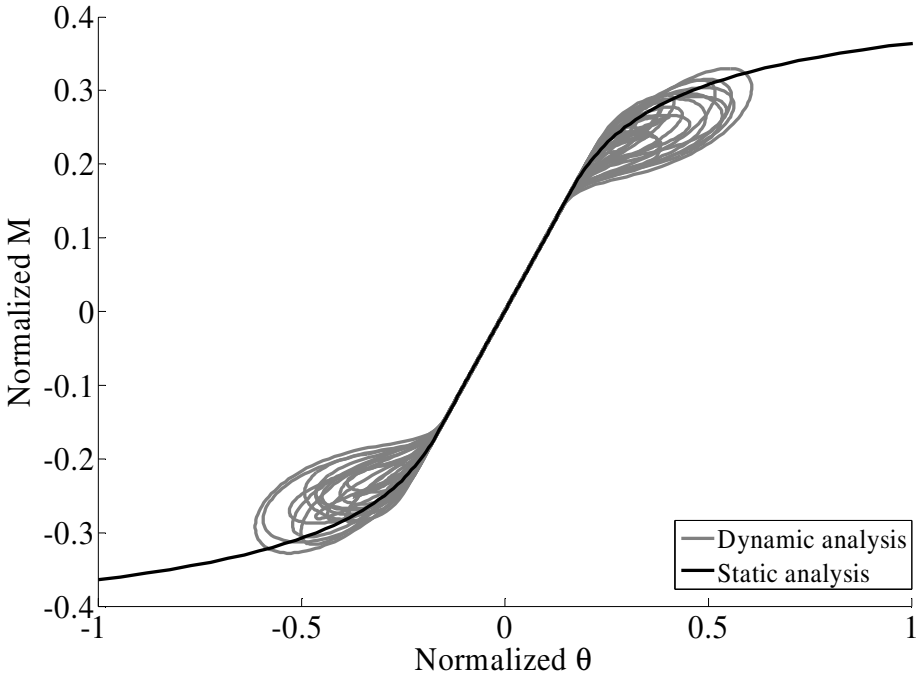


( a )

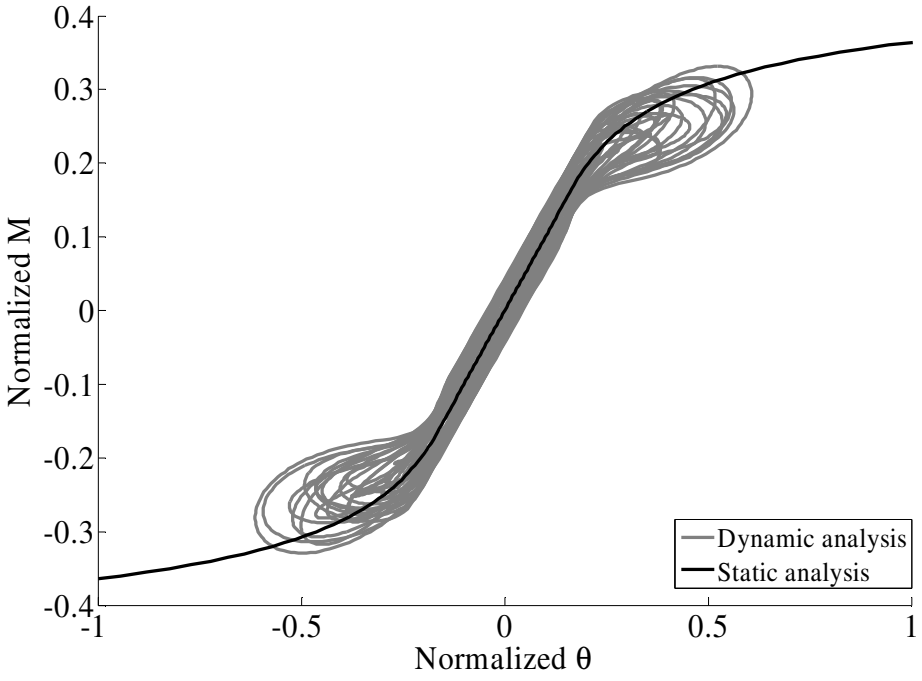


( b )

**Figure 3.4.** Comparison of *M-θ* response in dynamic analysis with that in static analysis for short period excitation by (a) employing equation 2.6, (b) employing equation 3.1.

In order to investigate the significance of vertical oscillations, the variation of $v$ normalized by static settlement (i.e., $V/K_v(B,L)$) with normalized $\theta$ is plotted in Figure 3.5. It is apparent that foundation uplift induces significant vertical oscillations, which in turn result in significant deviation of $M$-$\theta$ response of foundation from the static backbone curve. The vertical oscillations are rather important when separation of uplift becomes more pronounced.

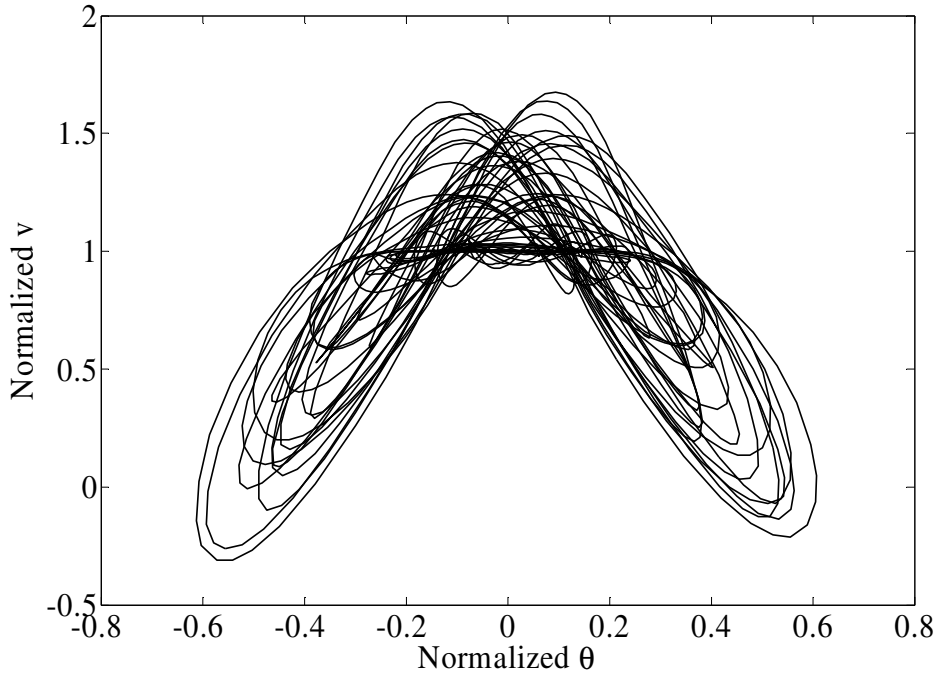


**Figure 3.5.** Variation of $v$ with $\theta$ during short period excitation.

In order to examine significance of error induced in estimation of $B'$ in deviation of $M$-$\theta$ relationship, the damping coefficients of foundation are multiplied by six in the analysis with short period excitation. The $M$-$\theta$ curves are presented in Figure 3.6. Although viscous reaction forces are more pronounced than the case shown in Figure 3.4, $M$-$\theta$ curves obtained by employing equation 2.6 follows the static backbone curve more closely than the foundation with lower damping. Hence, the main reason of deviation from static $M$-$\theta$ curve and fluctuations in $M$-$\theta$ relationship for larger amplitudes of excitation is the vertical oscillations

induced during uplift, because an increased $C_v$ results in reduced amplitudes of vertical oscillations and less diversion from static $M$-$\theta$ curve.

In order to verify the explanation for observed hysteretic loops in Figure 3.4.a, the deviation of dynamic vertical response and rocking response of foundation from static response is plotted in Figure 3.7. For that purpose, $\Delta\theta$, which is the difference between foundation rotation computed in dynamic response analysis and foundation rotation that corresponds to the same $M$ in static analysis, and $\Delta v$, which is the difference between vertical foundation displacement computed in dynamic response analysis and vertical foundation displacement that corresponds to the same $M$ in static analysis, is computed at each time-step. It is observed that, a relative increase in vertical displacement with respect to static displacement results in stiffer response in rocking mode, such that for any given instantaneous value of $M$, a decrease in rotation with respect to its static counterpart occurs. In contrast, a relative decrease in vertical displacement results in a relative increase in rotation.

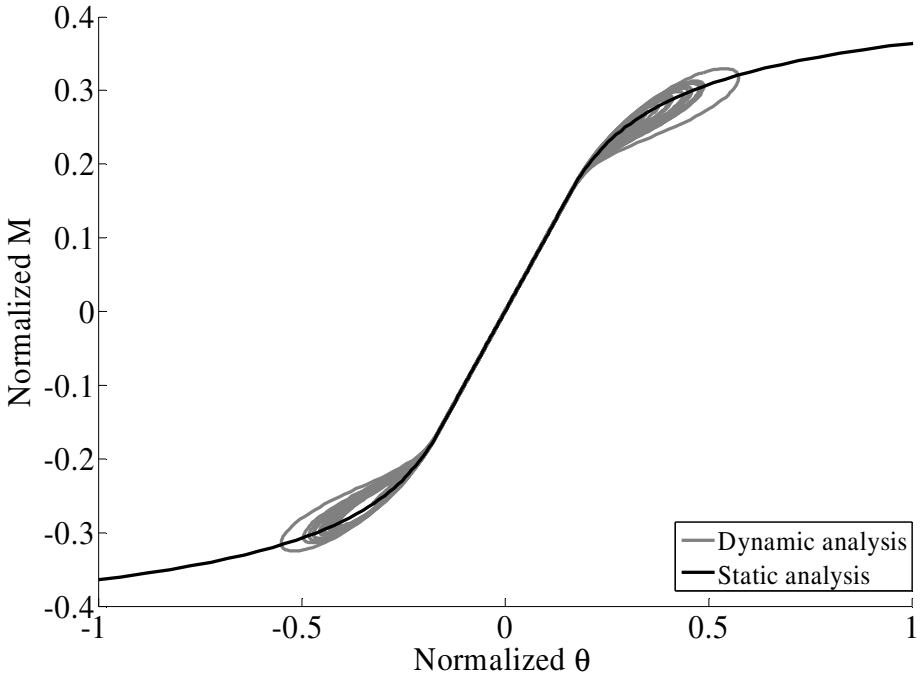


( a )

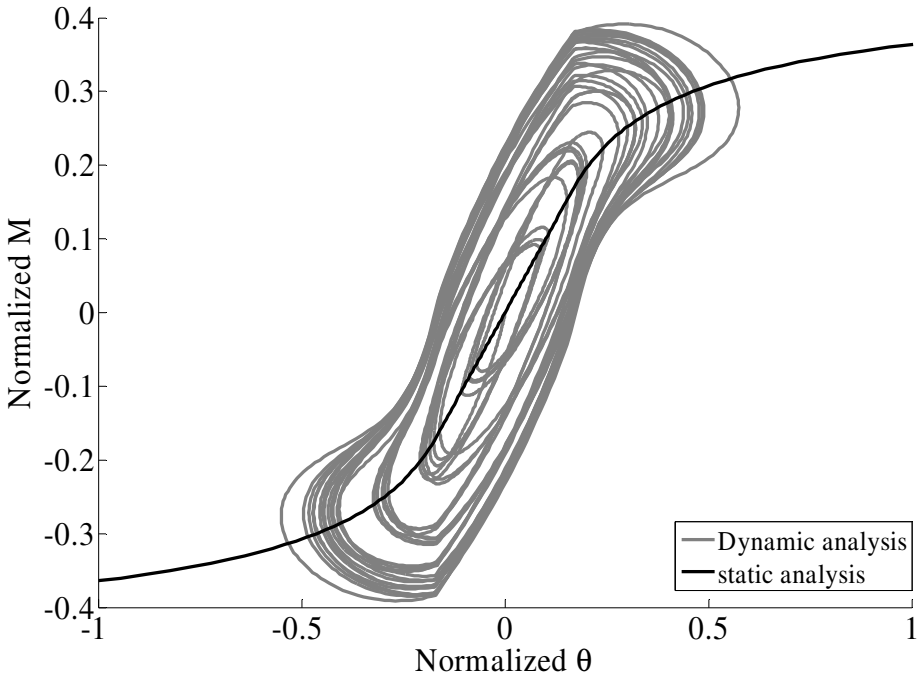


( b )

**Figure 3.6.** Comparison of *M-θ* response in dynamic analysis with that in static analysis for short period excitation and increased foundation damping by (a) employing equation 2.6, (b) employing equation 3.1.

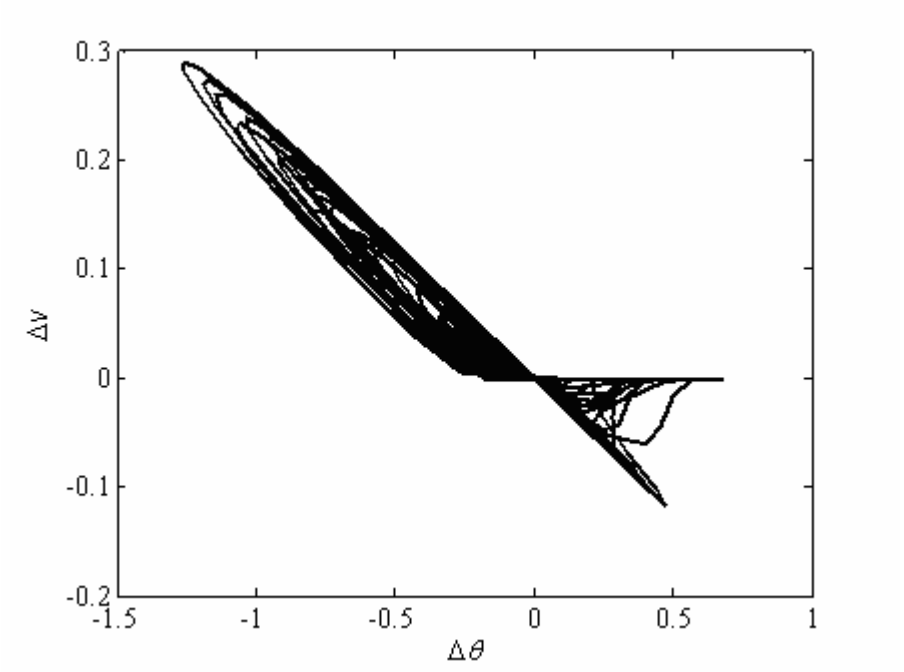


**Figure 3.7.** The deviation of dynamic response of a shallow foundation from its static response during short period excitation.

The transmission of energy between rocking and vertical modes of oscillations can be shown by integration of work done by reaction forces acting on the base of foundation. Hence, the work done by overturning moment till i$^{th}$ time step, $t_i$, is

$$W_M(t_i) = \int_0^{t_i} M(t) \cdot \dot{\theta}(t) \cdot dt \cong \sum_{j=1}^{i} \left( \left( \frac{M(t_j) + M(t_{j-1})}{2} \right) \cdot \left( \theta(t_j) - \theta(t_{j-1}) \right) \right) \qquad (3.20.a)$$

and the work done by vertical reaction force is

$$W_V(t_i) = \int_0^{t_i} V(t) \cdot \dot{v} \, dt \cong \sum_{j=1}^{i} \left( \left( \frac{V(t_j) + V(t_{j-1})}{2} \right) \cdot \left( v(t_j) - v(t_{j-1}) \right) \right) \qquad (3.20.b)$$

Figure 3.8 shows the history of $W_M$, $W_V$ and the total work done by foundation reaction forces, $W_M$+$W_V$, when contribution of viscous reaction forces in $M$ and $V$ are omitted. The work is normalized by $V^2/K_v(B,L)$ in Figure 3.8. The hysteretic

loops in $M$-$\theta$ plot (Figure 3.4.a) result in positive accumulation of $W_M$ by time, showing energy loss in rocking mode during successive load cycles. In contrast, the loops following counter-clockwise direction in $V$ - $v$ plot (Figure 3.9) exhibit accumulation of negative work done by vertical load, and an equivalent energy gain in vertical oscillation mode. The total work history is giving a mean zero process in Figure 3.8, showing that the overall response of foundation is elastic, but energy transmission between two modes of foundation oscillations occur due to coupling of $v$ and $\theta$ during uplift, and accurate simulation of vertical oscillations is mandatory.

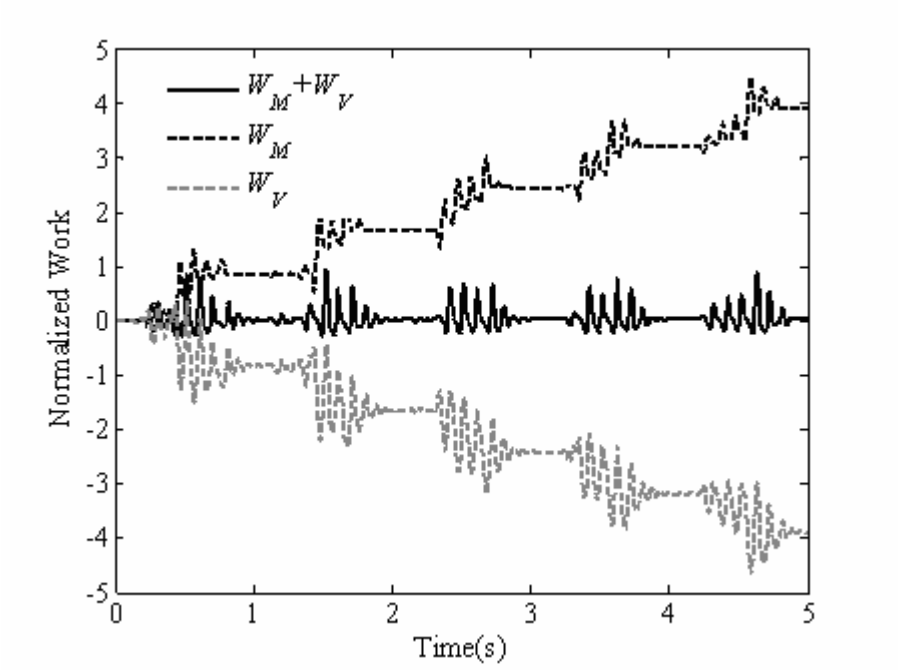


**Figure 3.8.** The work done by $M$ and $V$ during dynamic response to short period excitation.

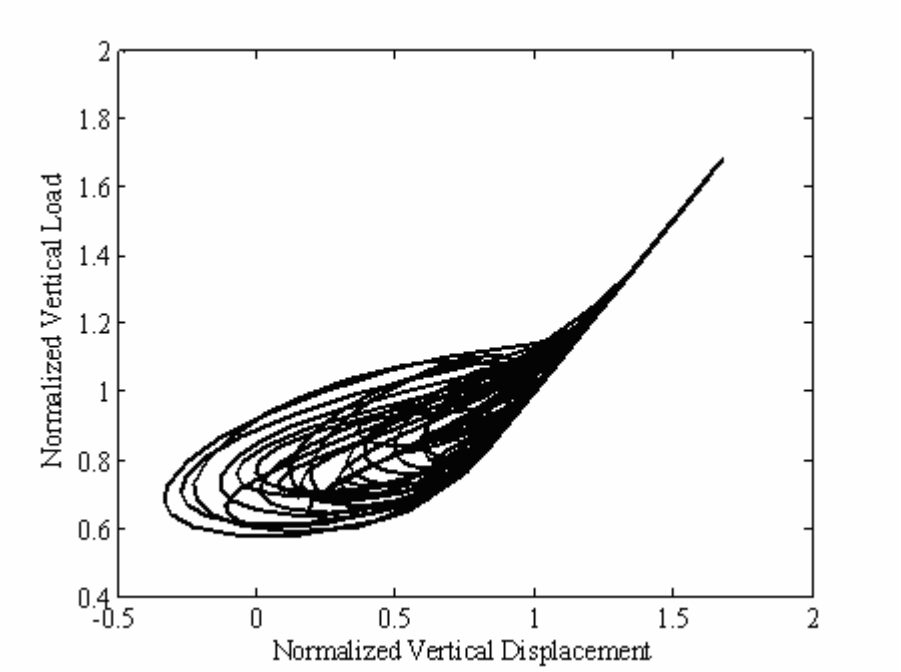


(a)

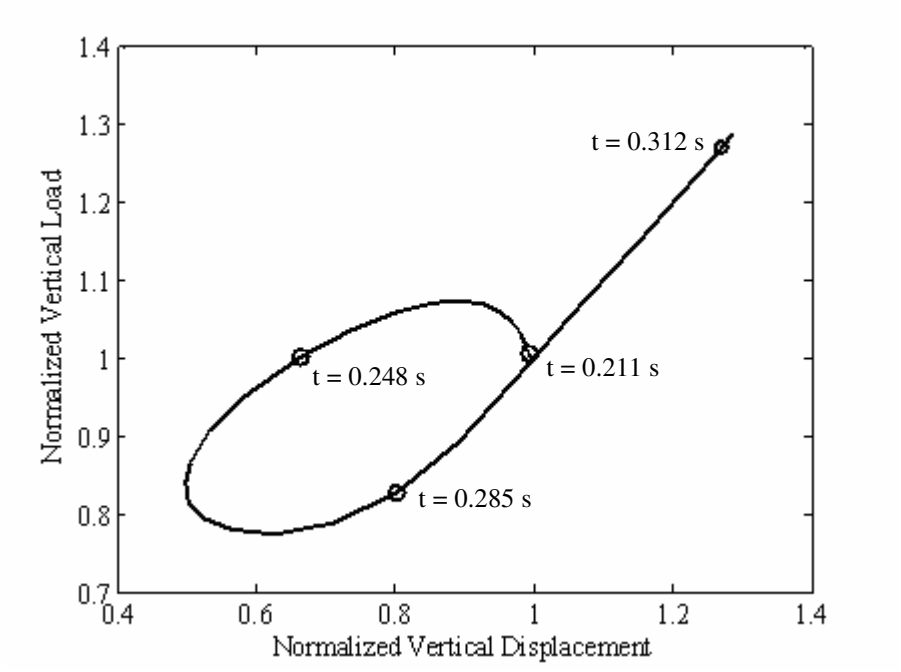


(b)

**Figure 3.9.** The *V-v* response of shallow foundation to short period excitation between time instants (a) 0 and 5 s, and (b) 0.211 and 0.312 s.

### 3.3.3 Response to Short Period, Large Amplitude Excitation

Finally the response of Winkler foundation to short period-large amplitude excitation is investigated. Large hysteretic loops in $M$-$\theta$ response point out very significant vertical displacements and excessive energy dissipation during uplift (Figure 3.10.a). This is also confirmed by Figure 3.11 that shows variation of $v$ with $\theta$: since excessive vertical displacements play a significant role in calculation of $B'$, the limitation of Winkler model that it cannot simulate vertical and rocking impedance of shallow foundation simultaneously renders a reduction in its capability to simulate uplift response of foundations.

No convergence problems arose during analyses, although contact width of foundation is decreased to levels less than % 20 of total width of rectangular foundation (Figure 3.12). The observation of increasing B´ by decreasing $\theta$ is possible when $v$ is also simultaneously increasing. Hence, accurate calculation of vertical foundation impedance is important for analysis of uplift problems. This issue is more important in analysis of frame structures, since vertical displacements of spread foundations are also constrained by structural frame, such that vertical load acting on a footing is dependent on its vertical displacement.

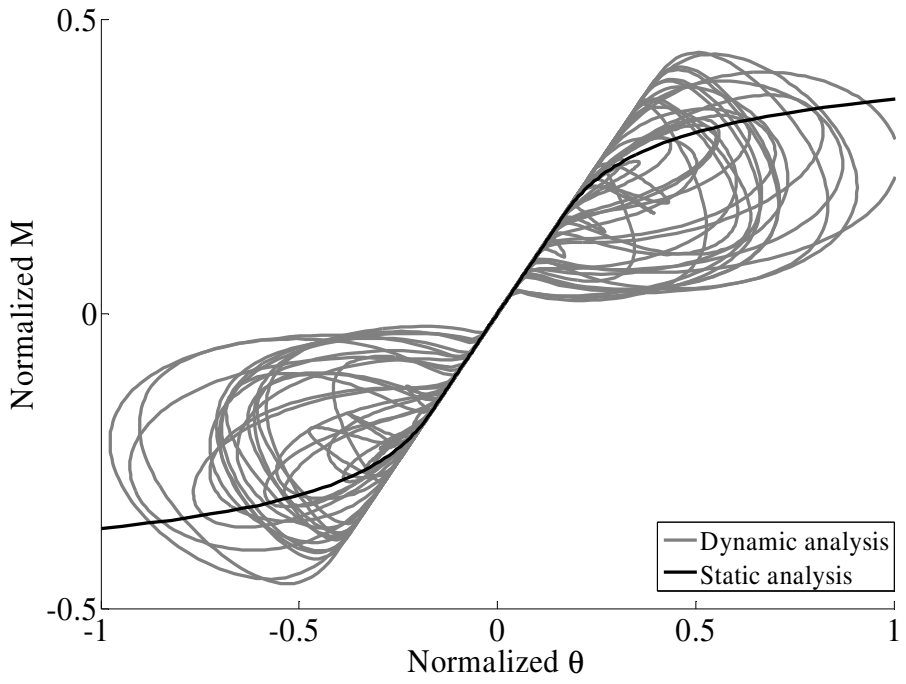


( a )

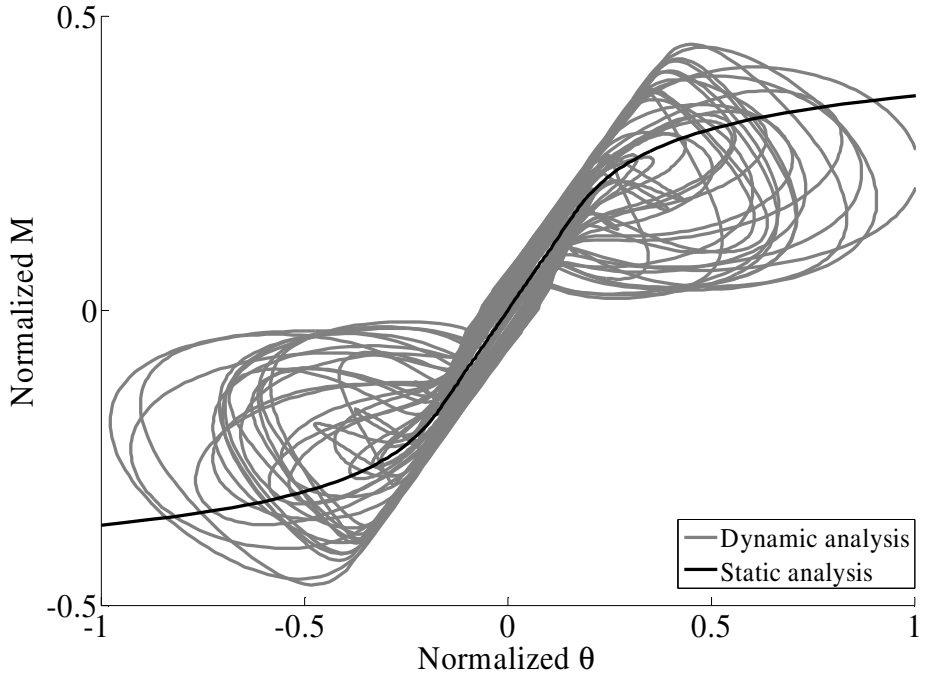


( b )

**Figure 3.10.** Comparison of $M$ - $\theta$ response in dynamic analysis with that in static analysis for short period-large amplitude excitation (a) employing equation 2.6, (b) employing equation 3.1

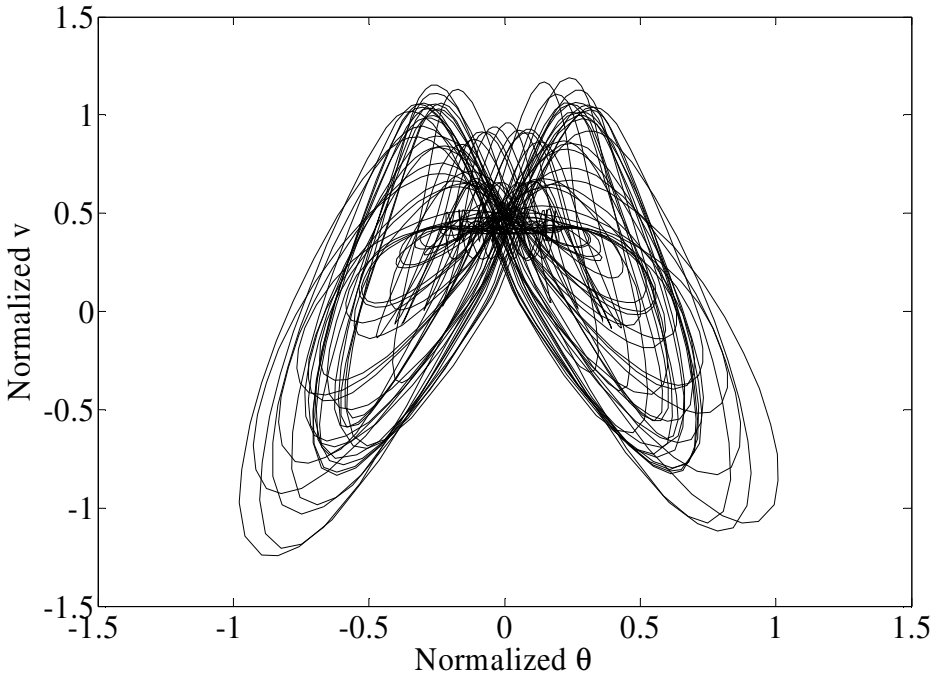


**Figure 3.11.** Variation of $v$ with $\theta$ during short period-large amplitude excitation.

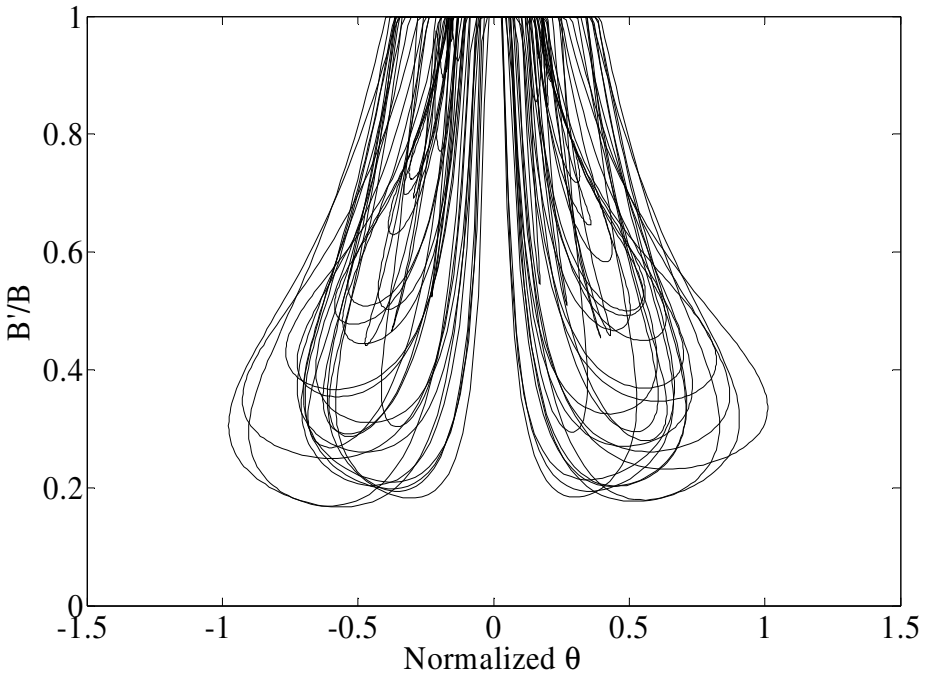


**Figure 3.12.** Variation of contact width with $\theta$ during short period-large amplitude excitation.

Finally time-histories of $u_t$, $u$, and $h \cdot \theta$ under short period-large amplitude excitation are presented in Figure 3.13. Although maximum amplitude of structural distortions during successive load cycles is somewhat constant, the total displacement amplitude of mass significantly increases due to uplift of foundation. In contrast with the results given in Figure 3.3, sharp peaks of $u$ can be observed, due to frequency content of excitation.

In summary, the results of both static and dynamic analyses show that, vertical response of foundation should be realistically modeled for accurate simulation of foundation uplift during seismic loading. Although Winkler model is useful for investigation of effect of foundation uplift on structural response, its inability to simulate vertical and horizontal reaction of a shallow foundation concurrently limits the realism in structural response computations that employ Winkler model.

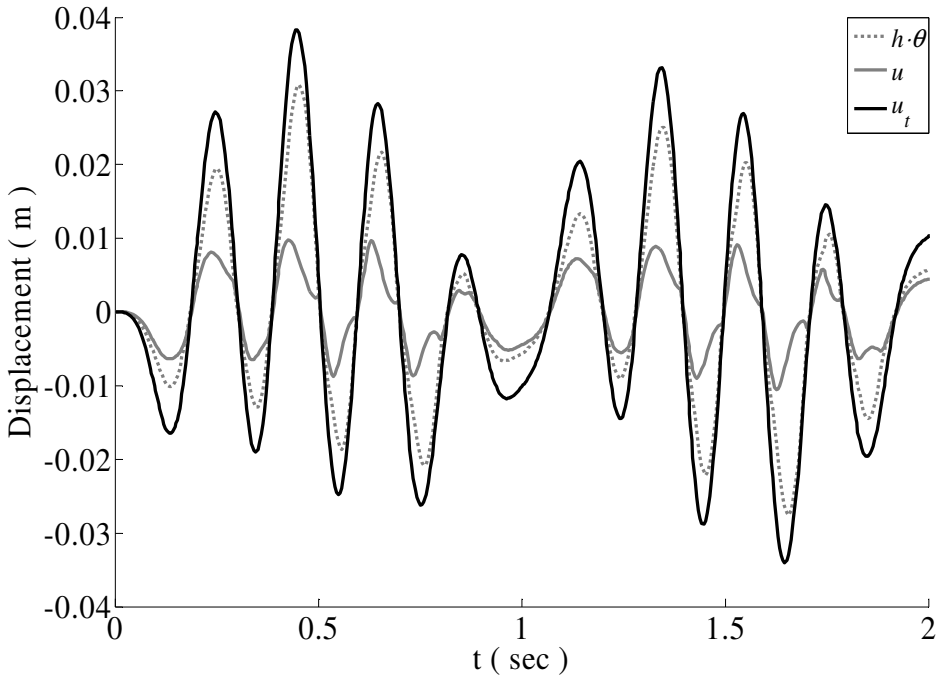


**Figure 3.13.** Comparison of $u_t$, $u$ and $h \cdot \theta$ histories for short period-large amplitude excitation.

# CHAPTER 4

# SUMMARY AND CONCLUSIONS

## 4.1. Summary

Uplifting of foundations can have an important role in seismic response of slender structures, such as towers, chimneys and bridge piers due to the increase in support flexibility. Calculation of nonlinear moment-rotation ($M - \theta$) relationship for footings of a frame structure is particularly important for investigation of damage susceptibilities of individual frame elements. Hence, realistic modeling of behavior of uplifting foundation is necessary. In this study, two algorithms are developed in order to compute static $M - \theta$ relationship for foundations during uplift, and to compute dynamic response of a simple inversed pendulum structure on tensionless foundation. Since Winkler model, which is described as a rigid foundation resting on distributed uniform tensionless springs, is widely employed in literature, the algorithms are used for critical evaluation of Winkler model. Hence response of a Winkler foundation is compared with that on elastic half-space through employing impedance factors given in literature.

The stiffness matrix of shallow foundation during uplift has been formulated as a function of the contact width and length. Assuming that the threshold moment for initiation of uplift is proportional to ultimate moment that can be exerted on a foundation on rigid base, fixed point iteration method with underrelaxation technique has been used to calculate the contact width. The vertical and rocking stiffness coefficients for a foundation on elastic half-space have been separately used for calculation of Winkler spring coefficients. Considering two different spring coefficients, the normalized $M - \theta$ relationship of Winkler model is

compared with that of foundation on elastic half-space.

In order to estimate the dynamic response of an inversed pendulum structure during foundation uplift, a second algorithm, based on Runge-Kutta method for solution of initial value problem at hand, has been developed by employing the dynamic equilibrium equations. The stiffness and damping matrices are calculated externally so that any type of support beneath the foundation can be easily introduced. The algorithm is used for computing response of an inversed pendulum structure on Winkler foundation. Considering a set of parameters, the dynamic $M$ - $\theta$ response of foundation is also compared with static $M$ - $\theta$ curve.

### 4.2. Conclusions

The following conclusions on analysis of foundation uplift have been obtained:

1- $M - \theta$ relationship for a foundation on elastic support is similar for the cases $\alpha$ = 1/2 and $\alpha$ = 1/3. Provided that experimental studies do not show that $\alpha$ should take a very distinct value, $\alpha$= 1/3, implicitly presumed by Winkler model, is a suitable choice for practical applications.

2- $M - \theta$ relationship of a Winkler foundation is significantly different from that of a foundation on elastic half-space, especially when vertical stiffness of foundation is employed for calculation of Winkler spring coefficients. When there is no constraint on vertical displacements, $k_0 = k_{0\theta}$ is the appropriate choice for Winkler spring coefficients.

3- The difference between $M - \theta$ relationship for Winkler model and for elastic half-space decreases when $\alpha$ increases.

4- The ratio $L/B$, hence the foundation geometry, has insignificant effect on normalized $M - \theta$ relationships.

5- When the nonlinear response of foundation becomes more prominent, the maximum structural distortion to total displacement ratio of an inversed pendulum structure decreases.

6- Increase in amplitudes of vertical oscilations during dynamic loading results in significant deviations from static $M - \theta$ curve. Hence, the capability of Winkler model to simulate uplift response is very limited since it cannot simulate the vertical and rocking impedance of a foundation consistently.

### 4.3. Future Studies

It is possible to introduce the nonlinearity of soil behavior in calculation of soil impedance factors. In literature, the nonlinear behavior of typical soils encountered in practice is presented with charts of shear modulus versus shear strain. Hence, through developing a constitutive model for foundation behavior such that a link between nonlinear response of soil and foundation is provided, a more rigorous method to compute $M - \theta$ relationship for a shallow foundation is possible.

The coupling between vertical displacement and rocking of foundation during uplift can have pronounced effect on the uplift performance of footings. Hence, limitations of existing practical procedures, which are generally based on Winkler model, for determination of structural response to foundation uplift can be critically investigated through employing the algorithms presented in this study.

# REFERENCES


Anderson D. L. (2003). Effect of foundation rocking on the seismic response of shear walls , Canadian Journal of Civil Engineering , 30 , 360–65.

Celep Z. and Güler K. (1990). Dynamic response of a column with foundation uplift, *Journal of Sound and Vibration*, 149, 2, 285–96.

Chapra S. C. and Canale R. P. (2006). *Numerical methods for Engineers, Fifth edition*, McGraw Hill International Edition.

Chen X. C. and Lai Y.-M. (2003). Seismic response of bridge piers on elasto-plastic Winkler foundation allowed to uplift, *Journal of Sound and Vibration*, 266, 957-96.

Chopra A. K. and Yim S. C.-S. (1985). Simplified earthquake analysis of structures with foundation uplift, *Journal of Structural Engineering*, 111, 4, 906-30.

Chopra A. K. (2007). *Dynamics of Structures – Theory and Applications to Earthquake Engineering, Third edition*, Pearson Prentice Hall.

Cook R. , Malkus D. S. , and Plesha M. E. (1989). *Concepts and Applications of Finite Element Analysis, Third edition*, Wiley.

Gazetas G. (1991). Formulas and charts for impedances of surface and embedded foundations, *Journal of Geotechnical Engineering*, 117, 9, 1363-81.

Harden H. , Hutchinson T. , and Moore M. (2006). Investigation into the the effects of foundation uplift on simplified seismic design procedures, *Earthquake Spectra*, 22, 3, 663–92.

Huckelbridge A. A. and Clough R. W. (1978). Seismic response of uplifting building frame, *Journal of The structural Division*, 104, No. ST8, 1211-22.

McCallen D. B. and Romstad K. M. (1994). Non-linear model for building–soil systems, *Journal of Engineering Mechanics*, 120 , 5, 1129-52.

Mergos P. E. And Kawashima K. (2005). Rocking isolation of typical bridge pier on spread foundation, *Journal of Earthquake Engineering*, 9, 2, 395–414.

Oliveto G. , Calio I. , and Greco A. (2003). Large displacement behaviour of a structural model with foundation uplift under impulsive and earthquake excitations, *Earthquake Engineering and Structural Dynamics*, 32, 369–93.

Psycharis I. N. (1991). Effect of base uplift on dynamic response of SDOF structures, *Journal of Structural Engineering*, 117, 3, 733–54.

Psycharis I. N. (2007). Investigation of the dynamic response of rigid footings on tensionless Winkler foundation, *Soil Dynamics and Earthquake Engineering*, doi: 10. 1016 / j. soildyn. 2007. 07. 010.

Roeder W. , Eeri M. , Banerjee S. , Jung D. R. , and Smith S. K. (1996). The role of building foundations in seismic retrofit, *Earthquake Spectra*, 12, 4, 925-42.

Song and Lee (1993). An improved 2-Spring model for foundation uplift analysis, *Computers and Structures*, 46, 5, 791–805.

Wang X.-F. and Gould P. L. (1993). Dynamics of structures with uplift and sliding, *Earthquake Engineering and Structural Dynamics*, 22, 12, 1085–95.

Wolf J. P. (1976). Soil – structure interaction with separation of base mat from soil ( Lifting – off ), *Nuclear Engineering and Design,* 38, 357–84.

Wolf J. P. and Skrikerud P. E. (1978). Seismic excitation with large overturning moments: Tensile capacity, projecting base mat or lifting–off, *Nuclear Engineering and Design*, 50, 305–81.

Xu C. and Spyrakos C. C. (1996). Seismic analysis of towers including foundation uplift, *Engineering Structures* , 18, 4, 271–78.

Yılmaz M. T. (2004). *Seismically induced tilting potential of shallow mats on fine soil , Ph. D. Thesis,* Middle East Technical University.

Yim S. C.–S. and Chopra A. K. (1984). Dynamics of structures on two-spring foundation allowed to uplift, *Journal of Engineering Mechanics*, 110, 7, 1124–46.